Early-life stress lastingly alters the neuroinflammatory response to amyloid pathology in an Alzheimer's disease mouse model

Hoeijmakers, L.; Ruigrok, S.R.; Amelianchik, A.; Ivan, D.; van Dam, A.-M.; Lucassen, P.J.; Korosi, A.

DOI
10.1016/j.bbi.2016.12.023

Publication date
2017

Document Version
Final published version

Published in
Brain, behavior, and immunity

Brain, Behavior, and Immunity 63 (2017) 160–175

Contents lists available at ScienceDirect

Brain, Behavior, and Immunity

journal homepage: www.elsevier.com/locate/ybrbi

Special Issue on Perinatal Inflammation

Early-life stress lastingly alters the neuroinflammatory response to amyloid pathology in an Alzheimer's disease mouse model

Lianne Hoeijmakers [a], Silvie R. Ruigrok [a], Anna Amelianchik [a], Daniela Ivan [a], Anne-Marie van Dam [b], Paul J. Lucassen [a,#], Aniko Korosi [a,*,#]

[a] Swammerdam Institute for Life Sciences, Center for Neuroscience, University of Amsterdam, Science Park 904, Amsterdam, The Netherlands
[b] Department of Anatomy & Neurosciences, Amsterdam Neuroscience, VU University Medical Center, De Boelelaan 1108, Amsterdam, The Netherlands

ARTICLE INFO

Article history:
Received 15 September 2016
Received in revised form 12 December 2016
Accepted 23 December 2016
Available online 25 December 2016

Keywords:
Early life
Stress
Neuroimmune
Microglia
Alzheimer's disease
Inflammation
Amyloid
Hippocampus

ABSTRACT

Exposure to stress during the sensitive period of early-life increases the risk to develop cognitive impairments and psychopathology later in life. In addition, early-life stress (ES) exposure, next to genetic causes, has been proposed to modulate the development and progression of Alzheimer's disease (AD), however evidence for this hypothesis is currently lacking. We here tested whether ES modulates progression of AD-related neuropathology and assessed the possible contribution of neuroinflammatory factors in this.

We subjected wild-type (WT) and transgenic APP/PS1 mice, as a model for amyloid neuropathology, to chronic ES from postnatal day (P)2 to P9. We next studied how ES exposure affected; 1) amyloid β (Aβ) pathology at an early (4 month old) and at a more advanced pathological (10 month old) stage, 2) neuroinflammatory mediators immediately after ES exposure as well as in adult WT mice, and 3) the neuroinflammatory response in relation to Aβ neuropathology.

ES exposure resulted in a reduction of cell-associated amyloid in 4 month old APP/PS1 mice, but in an exacerbation of Aβ plaque load at 10 months of age, demonstrating that ES affects Aβ load in the hippocampus in an age-dependent manner. Interestingly, ES modulated various neuroinflammatory mediators in the hippocampus of WT mice as well as in response to Aβ neuropathology. In WT mice, immediately following ES exposure (P9), Iba1-immunopositive microglia exhibited reduced complexity and hippocampal interleukin (IL)-1β expression was increased. In contrast, microglial Iba1 and CD68 were increased and hippocampal IL-6 expression was decreased at 4 months, while these changes resolved by 10 months of age. Finally, Aβ neuropathology triggered a neuroinflammatory response in APP/PS1 mice that was altered after ES exposure. APP/PS1 mice exhibited increased CD68 expression at 4 months, which was further enhanced by ES, whereas the microglial response to Aβ neuropathology, as measured by Iba1 and CD11b, was less prominent after ES at 10 months of age. Finally, the hippocampus appears to be more vulnerable for these ES-induced effects, since ES did not affect Aβ neuropathology and neuroinflammation in the entorhinal cortex of adult ES exposed mice.

Overall, our results demonstrate that ES exposure has both immediate and lasting effects on the neuroinflammatory response. In the context of AD, such alterations in neuroinflammation might contribute to aggravated neuropathology in ES exposed mice, hence altering disease progression. This indicates that, at least in a genetic context, ES could aggravate AD pathology.

1. Introduction

Alzheimer's disease (AD) is a highly prevalent, age-related neurological disorder characterized by a progressive deterioration of cognitive functions and the accumulation of specific neuropathological hallmarks, like amyloid β (Aβ)-containing plaques and neurofibrillary tangles in various brain regions (Querfurth and LaFerla, 2010). Next to specific genetic factors, like APP or PS1, AD etiology

Abbreviations: Aβ, amyloid β; AD, Alzheimer's disease; CA, cornu ammonis; Ctrl, control; DG, dentate gyrus; EC, entorhinal cortex; ES, early-life stress; IL, interleukin; LPS, lipopolysaccharide; ML, molecular layer; P, postnatal day; SML, stratum lacunosum-moleculare; SR, stratum radiatum; WT, wild-type.

* Corresponding author.
E-mail address: a.korosi@uva.nl (A. Korosi).
Shared senior author.

http://dx.doi.org/10.1016/j.bbi.2016.12.023
0889-1591/

and progression is influenced by environmental factors (Mayeux and Stern, 2012; Reitz and Mayeux, 2014). Of interest in this respect is that high levels of (perceived) stress have been previously associated with a stronger cognitive decline and increased AD incidence (Johansson et al., 2013; Kaplan et al., 2001; Katz et al., 2016; Lupien et al., 1999; Wilson et al., 2003).

These epidemiological studies are consistent with preclinical work showing that adult stress (hormone) exposure could aggravate amyloid pathology in several Aβ-based mouse models for AD (Baglietto-Vargas et al., 2015; Dong et al., 2008; Green et al., 2006; Han et al., 2016; Jeong, 2006; Rothman et al., 2012), accompanied by increased cognitive impairments and reductions in synaptic plasticity (Grigoryan et al., 2014; Huang et al., 2015). In addition, clinical and preclinical studies have shown that exposure to early-life stress (ES), such as childhood abuse or parental neglect, is strongly associated with cognitive impairments throughout life (Chugani et al., 2001; Li et al., 2015; Mueller et al., 2010; Philip et al., 2015; Rice et al., 2008; Vallee et al., 1999). In fact, ES seems to affect many health outcomes across the life span (Price et al., 2013; Ravona-Springer et al., 2012; Tyrka et al., 2010; Wolkowitz et al., 2010) and can increase the vulnerability to develop age-related disorders, such as AD (Kaplan et al., 2001; Lahiri and Maloney, 2012, 2010; Mishra and Gazzaley, 2014; Price et al., 2013; Schury and Kolassa, 2012). While a few studies have shown that perinatal stress could modulate AD related neuropathology in mouse models (Lesuis et al., 2016; Sierksma et al., 2013), little is known about possible biological substrates.

One possible mechanism through which ES might affect AD-related neuropathology could be changes in the neuroinflammatory response that are mediated among others by microglia in the brain. In the developing and adult brain, microglia and inflammatory factors are in fact essential for the formation and maintenance of the neuronal network (Bilbo and Schwarz, 2012; Harry, 2013; Reemst et al., 2016; Schwarz and Bilbo, 2012). Large-scale genetic studies have further identified immune-related pathways as risk factors for AD (reviewed in Malik et al., 2015), highlighting the relevance of the inflammatory system in the context of AD. Indeed, both the involvement of inflammatory factors and microglial cells in AD neuropathology is well established, and progression of Aβ pathology occurs in close association with inflammatory changes, that are among others mediated by microglia in the brain (Cunningham, 2013; Heneka et al., 2015; Mhatre et al., 2015; Spangenberg and Green, 2017).

Microglial activation in the presence of Aβ neuropathology can have beneficial effects (Wang et al., 2015, 2016), and mediate e.g. internalization and clearance of Aβ peptides (Fu et al., 2012; Lee et al., 2010; Liu et al., 2010; Majumdar et al., 2007). Nonetheless, the lasting microglial response to Aβ pathology is rather complex, and both beneficial and detrimental consequences have been reported for progression of the neuropathology (Guillot-Sestier et al., 2015; Heppner et al., 2015; Mhatre et al., 2015).

Interestingly, several recent clinical studies have reported an elevation of pro-inflammatory factors after childhood adversities (Baumeister et al., 2015; Bücker et al., 2015; Coelho et al., 2014; Machado et al., 2015; Redlich et al., 2015; Tyrka et al., 2015). These findings are supported by preclinical studies showing that exposure to prenatal stress (Diz-Chaves et al., 2012; Gómez-González and Escobar, 2009) or to daily postnatal maternal separation in rodents (Delpech et al., 2016; Roque et al., 2014), alters cytokine expression and maturation of microglia in the rodent brain. Moreover, the pro-inflammatory response to lipopolysaccharide (LPS) in adulthood is exacerbated after prenatal exposure to stress (Diz-Chaves et al., 2012; Szczesny et al., 2014), suggesting a long-term sensitization, or 'priming', of microglia after exposure to stress early in life (Hoeijmakers et al., 2015, 2016).

We here address whether perinatal stress-related, persistent alterations in the neuroinflammatory response may contribute to a more vulnerable profile that can subsequently lead to an aberrant response to accumulating Aβ peptides, and ultimately modify the extent of Aβ neuropathology. To test this, we exposed mice to chronic ES from postnatal day (P)2 to P9 (Naninck et al., 2015; Rice et al., 2008), and investigated if ES: 1) modulates amyloid pathology in the hippocampus and the entorhinal cortex (EC) at an early (4 months) and an advanced (10 months) pathological stage in APP/PS1 transgenic mice; 2) affects neuroinflammatory mediators (i.e. microglia and cytokine expression) directly after exposure to chronic ES at P9, and in adult wild-type (WT) offspring of 4 and 10 months of age; and 3) affects the neuroinflammatory response to Aβ accumulation in APP/PS1 mice of the same ages.

2. Materials and methods

2.1. Mice and breeding

Bigenic APPswe/PS1dE9 hemizygous males on a C56Bl/6J background were used to model AD related amyloid pathology. These APP/PS1 mice express chimeric mouse/human mutated APP K595N/M596L (Swedish mutation) and PS1, carrying an exon 9 deletion, driven by the mouse prion promoter. For more details, see B6C3-Tg (APPswe,PSEN1dE9)85Dbo/Mmjax strain of the Jackson Laboratory. Survival of the APP/PS1 mice was monitored, as various APP overexpressor lines including the APP/PS1 line, were reported to die prematurely (Hsiao et al., 1995; Moechars et al., 1999). Indeed, APP/PS1 overexpression decreased mouse survival by 8.0% at 4 months of age, and by 37.1% at 10 months. This survival was not affected by ES (*Ctrl:* $N = 62$, *ES:* $N = 46$, *Log-rank test:* $\chi^2(1) = 0.060$, $p = 0.807$).

To standardize the perinatal environment, all experimental mice were bred in house. For breeding, 8–10 week old virgin female C57Bl/6J mice were purchased from Harlan Laboratories B.V. (Venray, The Netherlands) and habituated for one week to the breeding room. Two females were housed together with one male (C57Bl/6J for a P9 cohort, APP/PS1 for a P120 cohort) and after one week, breeding males were removed, and females housed in pairs for another week. Afterwards, pregnant females were single-housed in a cage with filtertop, standard bedding material and nesting material consisting of one square piece of cotton nesting material (5 × 5 cm; Technilab-BMI, Someren, The Netherlands), in a ventilated, airflow-controlled cabinet to ensure a stable, quiet environment. Birth of pups was monitored every 24 h in the morning between 8.00 and 9.00 AM. Litters born before 9.00 AM were assigned to P0 on the previous day.

Standard housing conditions included cage enrichment, ad libitum water and standard chow, a temperature range of 20–22 °C, and a 40–60 % humidity. Animals were kept on a standard 12/12 h light/dark schedule (lights on at 8 AM). After weaning at P21, all mice were housed with same-sex littermates, 2–4 mice/cage, under standard housing conditions. All experimental procedures were conducted according to the Dutch national law and European Union directives on animal experiments, and were approved by the animal welfare committee of the University of Amsterdam.

2.2. Early-life stress paradigm

The early-life stress (ES) paradigm consisted of limiting the nesting and bedding material from P2 to P9 as described previously (Naninck et al., 2015; Rice et al., 2008). On the morning of P2, dams were randomly assigned to the ES or control (Ctrl) condition. Litters were culled to six pups to ensure litters of 5 to 6 pups,

including at least one male and one female. Dams and pups were weighted and housed under Ctrl or ES conditions. Ctrl cages contained standard amounts of sawdust bedding and one square, cotton piece of nesting material (5 × 5 cm). The ES cage contained a small amount of sawdust bedding, a fine-gauge stainless steel mesh raised 1 cm above the cage floor, and half a square, cotton piece of nesting material (2.5 × 5 cm). Cages were covered with a filtertop, and left undisturbed in the cabinet. On the morning of P9, pups were moved to standard cages (adult cohorts) or sacrificed (P9 cohort). All P9 pups were weight on the morning of P9, revealing an ES-induced reduction in body weight gain (*Ctrl:* 3.40 ± 0.51, *ES:* 2.32 ± 0.58, $t(26) = 6.652$, $p < 0.001$) which was no longer present at 4 and 10 month of age, confirming the previously described effects of ES (Naninck et al., 2015). Bodyweight was furthermore not affected by APP/PS1 overexpression (4 months: *condition* $F(1,20) = 3.156$, *ns, genotype* $F(1, 20) = 1.538$, *ns, interaction* $F(1,20) = 0.419$, *ns*; 10 months: *condition* $F(1,54) = 2.619$, *ns, genotype* $F(1,54) = 1.143$, *ns, interaction* $F(1,54) = 0.338$, *ns*).

2.3. Tissue preparation

The experimental design of this study is depicted in Fig. 1. Briefly, Ctrl and ES animals were sacrificed at P9, 4 months or 10 months of age and tissue was harvested for either gene expression or immunohistochemical analyzes (Fig. 1).

To collect brain material for gene expression analyzes, P9 male pups (5 litters total: Ctrl N = 6, ES N = 6), 4 month old adults (11 litters total: Ctrl WT N = 6, Ctrl APP/PS1 N = 6, ES WT N = 6, ES APP/PS1 N = 4) and 10 month old adults (11 litters total: Ctrl WT N = 6, Ctrl APP/PS1 N = 6, ES WT N = 11, ES APP/PS1 N = 6) were sacrificed by fast decapitation within the first two hours of the light-phase. The brains and hippocampi were quickly dissected and snap-frozen on dry-ice. Brain tissue was stored at −80 °C to minimize RNA degradation until further processing. RNA was extracted from fresh frozen hippocampal (unilateral) tissue using the TRIzol method (Invitrogen) (Chomczynski and Sacchi, 2006). Reverse transcription of RNA to cDNA was performed using SuperScript® III Reverse Transcriptase (Invitrogen) and cDNA samples were afterwards stored at −20 °C.

To collect material for immunohistochemistry, transcardial perfusion was performed as previously described, with the same procedure for coronal sectioning of brain tissue in 4 (P9) or 6 (adults) parallel series to obtain an equal representation of each brain per series (Naninck et al., 2015). The experimental ages and numbers of animals per age-group were P9 male pups (8 litters total: Ctrl N = 8, ES N = 7), 4 month old adults (11 litters total: Ctrl WT N = 10, Ctrl APP/PS1 N = 9, ES WT N = 11, ES APP/PS1 N = 8) and 10 month old adults (14 litters total: Ctrl WT N = 8, Ctrl APP/PS1 N = 6, ES WT N = 9, ES APP/PS1 N = 4).

2.4. Immunohistochemistry for amyloid and microglial markers

Amyloid load was identified after immunohistochemical staining for Beta amyloid using a monoclonal antibody 6E10 (mouse anti-human Aβ 1-16, SIG-3932-1000, BioLegend) at 4 and 10 month of age in Ctrl and ES APP/PS1 mice. Microglial cells were characterized using immunohistochemistry for ionized calcium binding adaptor molecule 1 (Iba1), a marker for microglia/macrophages (rabbit anti-Iba1, 019-19741, Wako) at P9, 4 and 10 month old mice, and for CD68, a protein present in microglial/macrophage lysosomes and endosomes commonly used as marker for phagocytic microglia (rat anti-mouse CD68 clone FA-11, MCA1957, Serotec) at ages of 4 and 10 months. A parallel series of perfused brain tissues was used for each staining.

For 6E10 staining of the adult tissues, sections were premounted on pre-coated glass slides (Superfrost Plus slides, Menzel)

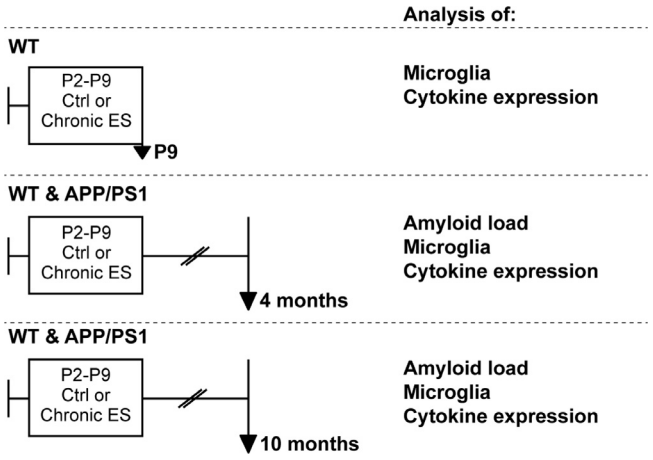

Fig. 1. Experimental design. Male C57Bl/6J (WT) and APPswe/PS1dE9 (APP/PS1) littermates were exposed to early-life stress (ES) from postnatal day (P)2 to P9 or control (Ctrl) condition. Afterwards, mice were either sacrificed directly after ES at P9 or in adulthood at 4 or 10 months of age to study microglia (protein and mRNA expression), cytokine mRNA expression and amyloid load.

and dried overnight while Iba1 and CD68 stainings were performed on free floating sections. 6E10 staining required pretreatment with citrate buffer to allow us to stain both for Aβ plaques as well as for cell-associated amyloid (also referred to as intracellular Aβ or pre-plaque peptides (Christensen et al., 2010). In between all staining steps, sections from P9 pup tissues and adult tissues used for 6E10 staining were washed in 0.05 M tris buffered saline containing 0.1% triton X-100 (TBS-tx, pH 7.6), and sections from adult brains used for microglial Iba1 and CD68 staining were washed in 0.05 M TBS. After washing, sections were incubated in 0.3% H_2O_2 for 15 min to block endogenous peroxidase activity. For the 6E10 stainings, this was followed by pretreatment with 0.01 M citrate buffer pH 6.0 for 15 min in a microwave, set to reach and maintain a temperature of ±95 °C, after which they were allowed to cool to room temperature. Next, all sections were incubated for 30 min in blocking mix containing 1% bovine albumin serum (BSA) in 0.05 M TBS-tx. Primary antibodies were diluted (1:1500 6E10, 1:5000 Iba1 or 1:400 CD68) in blocking mix and incubated for 1 h at RT (Iba1, CD68) or 2 h at RT (6E10), followed by incubation at 4 °C overnight. Sections were incubated in the secondary antibodies, respectively 1:200 sheep anti-mouse biotinylated (GE Healthcare), 1:500 goat *anti*-rabbit biotinylated (Vector Laboratories) or 1:500 goat anti-rat biotinylated (Vector Laboratories) in blocking mix. After 2 h, sections were incubated with avidin-biotin complex 1:800 in 0.05 M TBS (Vectastain elite ABC-peroxidase kit, Brunschwig Chemie). Finally, sections were thoroughly washed in 0.05 M TB (pH 7.6) and incubated in 0.2 mg/1 ml diaminobenzidine (DAB), 0.01% H_2O_2 in 0.05 M TB) for the chromogen development. After DAB staining sections were rinsed in TBS and the free-floating sections were mounted on pre-coated glass slides (Superfrost Plus slides, Menzel) and all slides were cover slipped.

2.5. Quantification of amyloid load

All quantification procedures were performed by a researcher blind to the experimental conditions. For analysis of all stainings, 6 coronal sections of the hippocampus were selected between bregma −1.22 mm and bregma −3.64 mm, of which 3 bilateral sections between bregma −2.30 mm and bregma 3.64 mm were selected for analysis of EC. All sections had an approximate 320 μm (P9) or 480 μm (adult) intersection distance to obtain an

even presentation of the hippocampus over the rostral/caudal axis per animal per staining.

Amyloid load was quantified using a standard thresholding method for the analysis of amyloid plaque load and cell-associated amyloid as described before (Marlatt et al., 2013). 6E10 immunostained sections were imaged with a 10x objective on a Leica CTR5500 microscope using the Leica MetaMorph software. Images were processed using freely available ImageJ software (National Institutes of Health). First, the dentate gyrus (DG), cornu ammonis (CA) and EC were traced in all sections to determine the regions of interest, after which the images were converted to 8-bit black-white images. A threshold was set to select all 6E10 immunoreactive material, including both cell-associated amyloid staining and 6E10 plaques. The plaque load was then determined by specifically distinguishing 6E10 immunoreactive plaques from cell-associated amyloid using ImageJ's *analyze particles* plugin. Specifically, thresholded-immunoreactive material was identified as 6E10 plaque material when its surface was >140 μm^2 (exceeding cell sizes), after which the percentage of surface occupied by 6E10 plaque material within the region of interest (DG, CA or EC) was calculated to reflect the plaque load. Similarly, cell-associated amyloid was quantified as the number of immunoreactive cells, by counting the thresholded cells that were distinguished from the immunoreactive plaques based on the smaller surface (40–140 μm^2) and more circular shape (0.25–1.00).

2.6. Quantification of microglial markers Iba1 and CD68

2.6.1. Microglial density and coverage

P9 and adult immunostained tissue was processed for an estimation of the microglial coverage and density using thresholding (Beynon and Walker, 2012; Ziko et al., 2014).

In the P9 tissue, the Iba1 immunopositive staining in the DG was imaged with a 20x objective on a Zeiss Axiophot light microscope with Microfire camera (Coptronics) using StereoInvestigator software (MicroBrightField), Iba1 stained adult tissue was imaged using a 10x objective on a Nikon Eclipse Ni-E microscope using the Nikon Elements software and CD68 stained adult tissue was imaged using a 20x objective on a Leica CTR5500 microscope using the Leica MetaMorph software. We traced the DG, CA and EC, and additionally the molecular layer (ML) of the DG, stratum lacunosum-moleculare (SML) and stratum radiatum (SR) of the CA1 in the Iba1 immunostained adult brain sections, because these regions are primarily affected by amyloid deposition at 4 and 10 months. After tracing, images were converted to 8-bit black-and-white images and in addition for Iba1 staining in 10 month old mice only, background was subtracted. A fixed threshold was determined for each staining and age group to determine the percentage of immunoreactive stained area (coverage) in the respective regions. For adult tissue (4 and 10 months), a second threshold was used to identify the soma of the microglial cells and the number of the so identified cells was counted. Finally, because microglial Iba1 and CD68 cells that are clustered in 10 month old APP/PS1 mice with abundant neuropathology are not included in the estimation of individual microglial cell density, clustering of activated Iba1 and CD68 cells in 10 month old Ctrl and ES APP/PS1 mice was analyzed separately by selecting all immunoreactive (thresholded) area exceeding the single-cell size to obtain the coverage of clustered microglial cells. The selection criteria had been checked before ad random comparing some automated cell count results with separate manual quantifications for each experimental study.

2.6.2. Quantification of subtype specific microglial morphology and complexity

To determine whether changes in microglial coverage can be attributed to altered morphology and/or complexity of the Iba1 immunoreactive cells, we classified microglia based on their morphological appearance, and performed measurements of individual cells to identify changes in cell size and complexity in all age groups. In P9 pups, all microglia in the DG in 6 bilateral sections (see Section 2.3) were classified manually based on the morphology. In the age groups of 4 and 10 months, the cells used for individual cell measures in the hippocampus and the cells used for EC individual cell measures were also used to classify adult microglia. These individual cell measures were applied by selecting all microglia present in 4 frames of 234 μm by 302 μm which were placed in the hilus of the DG or in the EC (Roque et al., 2016) in 2 bilateral sections (N = 6 animals per group).

The morphological classification was performed by subdividing the cells in 4 morphological phenotypes; round/amoeboid, cells with stout processes, cells with thicker, longer processes and cells with thinner ramified processes as described previously (Schwarz et al., 2012). Examples of these cells are provided in Fig. 3C. Individual cells were furthermore characterized by tracing the outline of the cell to obtain a 2D cell surface, the soma diameter, and primary process number. Cells with overlapping somas or absence of the soma were excluded for the analysis. This provided a total of 25–36 (depending on the age group) analyzed cells per animal. These same cells were furthermore traced to perform Sholl analysis (Papageorgiou et al., 2016; Roque et al., 2016) using ImageJ in order to assess the complexity of the microglial processes. Virtual concentric circles where drawn at a 1 μm radius interval from the soma for a total distance of 60 μm and the number of traced process intersections were counted.

2.6.3. DG volume estimation

Volume estimations of the DG were obtained by applying Cavalieri's principle. The DG tracings in 6 bilateral sections were used to estimate the total surface (μm^2) of the DG and hippocampus in 6 bilateral sections, which was multiplied by the number of series (4 for pups, 6 for adult mice), section thickness (40 μm), and multiplied by 2 for the ratio of analyzed DG sections (6) from the total number of hippocampal sections within the series (12).

2.7. Gene expression measurement with RT-PCR

Relative gene expression of microglial activation markers was assessed by PCR amplification of cDNA using the Hot FirePol Evagreen qPCR supermix (Solis Biodyne), and measured using the 7500 Real-time PCR system (Applied Biosystems). Primer sequences for reference genes and genes of interest are listed in Table 1. Efficiency of primer pairs was tested prior to experimental use, requiring 90–110% efficiency.

Cytokine expression was measured using more sensitive taqman probes. Samples were processed with TaqMan® Universal Master Mix II with UNG (Applied Biosystems) using predesigned probes listed in Table 2, and measured using the 7500 Real-time PCR system (Applied Biosystems).

Multiple references genes were used for normalization of both the Evagreen and TaqMan probe experiments, following the

Table 1
Primer sequences for RT-PCR.

Target gene	Forward primer (5′-3′)	Reverse primer (5′-3′)
RPL13a	CCCTCCACCCTATGACAAGA	TCGCCTGTTTCCGTAACCTC
RPL0	GCTTCATTGTGGGAGCAGACA	CATGGTGTTCTTGCCCATCAG
SDHA	GTTGCTGTGTGGCTGACTG	GCACAGTGCAATGACACCAC
Iba1	ACAAAGAACACAAGAGGCCAACT	TGTGACATCCACCTCCAATCAG
CD68	TGACAAGGGACACTTCGGG	GGAGGACCAGGCCAATGAT
CD11b	GGGTCATTCGCTACGTAATTGG	CGTGTTCACCAGCTGGCTTA

Table 2
Probes for TaqMan® RT-PCR.

Target gene	Probe reference
TBP	Mm00446973_m1
RPL0	Mm00725448_s1
IL-1β	Mm00434228_m1
IL-6	Mm00446190_m1
IL-10	Mm00439616_m1
TNFα	Mm00443258_m1

requirements for reference target stability quality control (M < 0.5, CV < 0.25), calculated using qBASE software (Biogazalle) (Derveaux et al., 2010; Hellemans et al., 2007). Relative gene expression was finally calculated using the $2^{\Delta\Delta ct}$ method, after normalization for 2 or 3 reference genes, which were not altered by experimental treatments. Selected reference genes: SDHA and RPL13A for P9 Evagreen experiments; RPL0, RPL13A and SDHA for Evagreen experiments with 4 month old mice; RPL0 and RPL13A for Evagreen experiments with 10 month old mice; RPL0 and TBP for all TaqMan probe experiments.

2.8. Statistical analysis

Data were analyzed using SPSS 20.0 (IBM software), Graphpad Prism 5 (Graphpad software), and SAS Business analytics software. Data are expressed as mean ± standard error of the mean (SEM). Data were considered statistically significant when $p < 0.05$. In each of the experiments, multiple mice from the same litters were included, therefore, models with litter included as a random factor were run to assess to which degree litter effects influenced the dependent variable. Litter effects were negligible for all variables.

Survival of Ctrl APP/PS1 and ES APP/PS1 mice was analyzed using the log-rank test. Data with only genotype or condition as independent factor were analyzed with unpaired Student's *t*-test. Data of adult bodyweight, DG volume, Iba1 cell density and coverage, CD68 cell density and coverage and gene expression data of adult mice were analyzed with two-way ANOVA (independent factors condition and genotype). If a significant interaction effect was detected, *post-hoc* analyzes were performed using Bonferroni multiple comparison tests.

Measurements of multiple cells within one animal (single-cell measures for soma diameter, number of primary processes and cellular surface at P9) were analyzed with the unpaired Student's *t*-test (independent factor condition) with animal included as a random factor. The influence of animal effects was negligible for most parameters, with the exception of soma diameter ($\chi^2(1) = 4.048$, $p = 0.044$). Sholl analysis of individual Iba1 microglia at P9, 4 months and 10 months was analyzed using repeated measures ANOVA with SAS Business analytics software with distance from soma as a repeated factor, animal included as a random factor and condition and genotype as independent factors.

3. Results

3.1. Reduced DG volume lasts into adulthood

Firstly, we assessed DG volume in WT mice at P9 and found that the volume of the DG is about 62.9% smaller directly after ES exposure (*Ctrl:* 3.40 ± 0.51, *ES:* 1.26 ± 0.13, $t(13) = 2.559$, $p = 0.024$). The volume of the DG tends to remain reduced in adult mice exposed to ES, irrespective of the genotype of the mice (4 months: *condition* $F(1,33) = 3.833$, $p = 0.059$, *genotype* $F(1,33) = 0.165$, *ns, interaction* $F(1,33) = 0.034$, *ns;* 10 months: *condition* $F(1,26) = 4.262$, $p = 0.049$, *genotype,* $F(1,26) = 0.268$, *ns, interaction* $F(1,26) = 0.268$, *ns*) confirming and expanding on earlier descriptions (Naninck et al., 2015). Therefore, all quantification of amyloid pathology, Iba1 and CD68 were expressed either as a percentage of the total area, or as cells per mm^2.

3.2. Amyloid pathology is reduced at 4, but aggravated at 10 months in the DG by ES

3.2.1. Cell-associated amyloid is reduced by ES at 4 months

Amyloid pathology at the early-pathological stage in 4 month old APP/PS1 mice consisted mostly of cell-associated amyloid, which is the most abundant form present at that age and only few Aβ plaques were present in the hippocampus and entorhinal cortex (Fig. 2A), confirming and extending previous descriptions (LaFerla et al., 2007). At this age, ES affected amyloid accumulation specifically reducing the cell-associated form in the DG by 66% while this was not altered in the CA or EC (Fig. 2B, C, D; DG; *Ctrl:* 25.38 ± 4.42, *ES:* 8.63 ± 2.08, $t(14) = 3.429$, $p = 0.004$; CA: *Ctrl:* 49.41 ± 4.60, *ES:* 36.23 ± 8.87, $t(14) = 1.318$, *ns*; EC: *Ctrl:* 115.90 ± 18.33, *ES:* 93.78 ± 20.36, $t(14) = 0.8091$, *ns*). Aβ plaque load was not affected in either DG or CA subregion of the hippocampus (Fig. 2E, F; DG: *Ctrl:* 0.04 ± 0.01, *ES:* 0.02 ± 0.01, $t(14) = 1.656$, *ns*; CA: *Ctrl:* 0.02 ± 0.00, *ES:* 0.01 ± 0.04, $t(14) = 0.851$, *ns*). In the entorhinal cortex, ES tended to reduce the plaque load, although this did not reach significance (Fig. 2G; *Ctrl:* 0.04 ± 0.01, *ES:* 0.02 ± 0.01, $t(14) = 1.828$, $p = 0.089$).

3.2.2. Aβ plaque load is elevated by ES at 10 months

Aβ plaque deposits were the most prominent form of Aβ pathology at a more advanced pathological stage in the 10 month old APP/PS1 mice in the hippocampus. The DG was the most severely affected region, and cell-associated amyloid was less abundant in the whole hippocampus at this age (Fig. 2H). While cell-associated amyloid was not significantly altered in the DG, CA or EC of ES exposed offspring (Fig. 2I, J, K; DG: *Ctrl:* 22.13 ± 2.77, *ES:* 28.22 ± 0.795, $t(8) = 1.732$, *ns*; CA: *Ctrl:* 14.77 ± 1.76, *ES:* 19.75 ± 2.96, $t(8) = 1.553$, *ns*; EC: *Ctrl:* 64.32 ± 19.29, *ES:* 119.70 ± 26.89, $t(14) = 1.722$, *ns*), Aβ plaque load was increased by 54.4% after ES exposure in the DG, but remained unaffected in the CA and EC at this age (Fig. 2L, M, N; DG: *Ctrl:* 0.68 ± 0.08, *ES:* 1.05 ± 0.09, $t(7) = 3.113$, $p = 0.017$; CA: *Ctrl:* 0.36 ± 0.06, *ES:* 0.34 ± 0.04, $t(8) = 0.302$, *ns*; EC: *Ctrl:* 1.16 ± 0.27, *ES:* 1.32 ± 0.17, $t(14) = 0.447$, *ns*).

3.3. Chronic ES exposure affects the neuroinflammatory response at P9

3.3.1. Iba1 microglial coverage and complexity are reduced in the DG after ES exposure

A detailed analysis of microglial Iba1 immunostaining in the DG of P9 WT Ctrl and ES pups was performed by quantifying immunostaining covered surface area (coverage), total and subtype-specific cell density and individual cell size and complexity (Fig. 3A). Iba1 coverage was reduced in ES mice (Fig. 3B, *Ctrl:* 22.93 ± 1.60, *ES:* 17.76 ± 1.34, $t(13) = 2.431$, $p = 0.030$), while the total density of Iba1 cell numbers, and the density of each subtype classified based on the morphology, were not affected by ES. (Fig. 3C Total; *Ctrl:* 341.40 ± 14.15, *ES:* 332.90 ± 13.54, $t(13) = 0.431$, *ns*; Ramified*: Ctrl:* 425.0 ± 38.76, *ES:* 423.7 ± 41.59, $t(13) = 0.023$, *ns;* Thick/long processes*: Ctrl:* 355.4 ± 19.93, *ES:* 330.3 ± 20.42, $t(13) = 0.877$, *ns;* Stout processes*: Ctrl:* 59.00 ± 6.49, *ES:* 62.14 ± 5.28, $t(13) = 0.369$, *ns;* Amoeboid*: Ctrl:* 19.86 ± 2.65, *ES:* 13.88 ± 3.00, $t(13) = 1.474$, *ns*).

Detailed analysis of individual cells showed that ES alters the Iba1 phenotype and leads to reduced Iba1 cell size and complexity in the hilus of the DG. Cellular surface of individual Iba1 cells was reduced by ES, while their soma diameter and number of primary processes were not affected by ES exposure (Cellular surface: *Ctrl:*

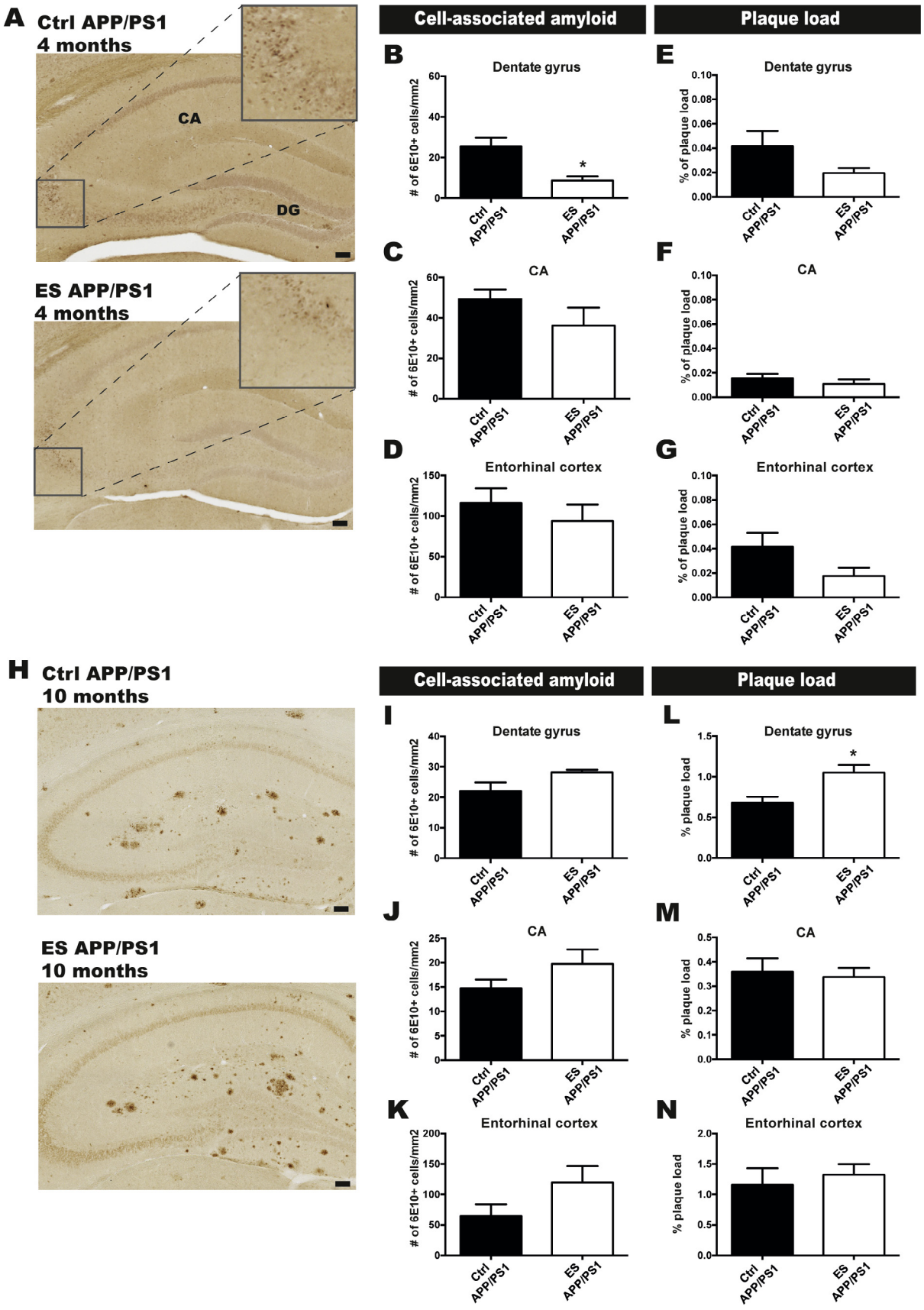

Fig. 2. Chronic ES modulates amyloid load in APP/PS1 mice in the dentate gyrus. A) Representative images of Aβ staining (6E10) in 4 month old Ctrl and ES APP/PS1 males, marking the dentate gyrus (DG) and cornu ammonis (CA). B) Cell-associated amyloid is decreased by ES exposure in the DG. C) In the CA and D) entorhinal cortex (EC), cell-associated amyloid is not affected by ES exposure. Plaque load in E) the DG, F) the CA as well as G) the EC is also not affected by ES in 4 month old APP/PS1 mice. H) Representative images of Aβ staining (6E10) in 10 month old Ctrl and ES APP/PS1 males. Cell-associated amyloid in I) the DG, J) the CA as well as K) the EC is not affected by previous exposure to ES. L) Aβ plaque load is increased in the DG after ES exposure in 10 month old males, M) but not in the CA or N) in the EC. Scale bar: A, H) 100 μm. *: condition effect.

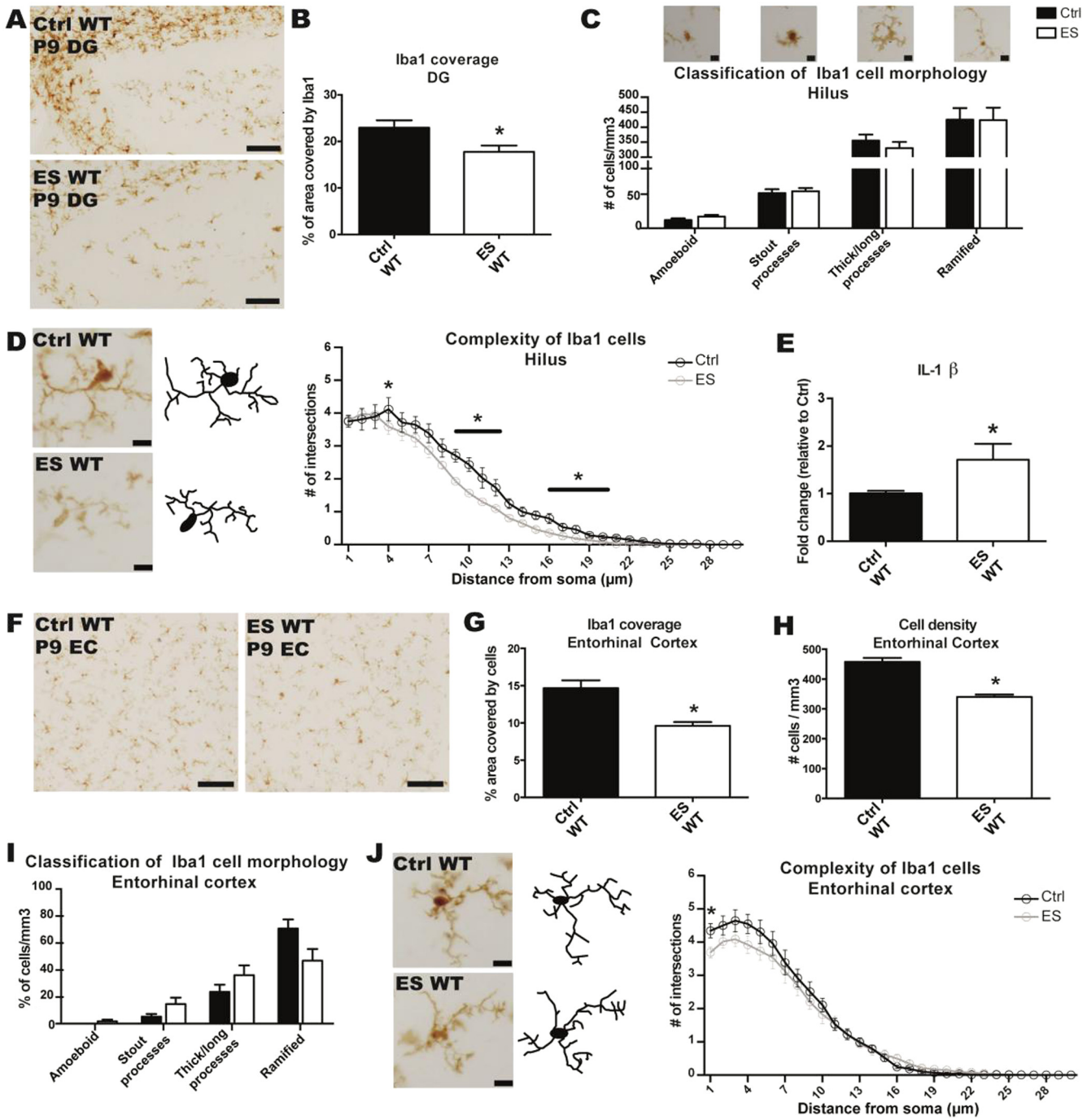

Fig. 3. Chronic ES exposure affects microglia and IL-1β mRNA expression in the hippocampus at P9. A) Representative images of Iba1 immunoreactive cells in P9 Ctrl and ES WT males in the dentate gyrus (DG). B) The coverage of Iba1 surface area is reduced by ES exposure. C) Quantification of microglial cell density and classification of corresponding morphological appearance shows no difference between Ctrl and ES animals. D) Two representative images of Ctrl WT and ES WT microglia in the hilus of the DG, with their respective tracing for Sholl analysis, indicating reduced complexity of ES microglia. This reduction is specifically present at 4 µm, 9 to 12 µm and from 16 to 20 µm from the soma. E) IL-1β mRNA expression in the hippocampus is increased by ES exposure. F) Representative images of Iba1 immunoreactive cells in P9 Ctrl and ES WT males in the entorhinal cortex (EC). G) Iba1 coverage and H) the density of Iba1 cells in the EC is reduced after ES. I) Classification of microglial morphological appearance shows no difference between Ctrl and ES animals. J) The complexity of Iba1 cells in the EC is not different between Ctrl and ES mice, with the exception of less primary dendrites in ES mice at P9. Scale bar: A,F) 100 µm, C,D,J) 10 µm. *: condition effect.

468.16 ± 158.02, *ES:* 386.00 ± 116.89, $t(11.999) = -2.861$, $p = 0.014$; Soma diameter: *Ctrl:* 8.54 ± 2.14, *ES:* 8.91 ± 2.30, $t(12.002) = 0.662$, *ns*; Primary process number: *Ctrl:* 4.24 ± 1.47, *ES:* 4.20 ± 1.34, $t(11.986) = -0.222$, *ns*). The reduction in individual cell surface was accompanied by a reduction in cellular complexity of the Iba1 cells. Sholl analysis revealed that ES specifically reduced the complexity of more distal branching of microglia of ES exposed offspring (Fig. 3D, *condition* $F(1,5449) = 8.76$, $p = 0.003$*; post-hoc: ES significant lower than Ctrl at* 4 µm, 9 *to* 12 µm, *and* 16 *to* 20 µm *from the soma*).

3.3.2. Microglial activation and cytokine expression in the hippocampus at P9

Expression of the pro-inflammatory cytokine interleukin (IL)-1β was increased by 69.3% after ES exposure (Fig. 3E, *Ctrl:* 1.01 ± 0.05, *ES:* 1.71 ± 0.33, $t(9) = 2.313$, $p = 0.046$), while the expression of the

cytokines IL-6, TNFα and IL-10, with pro- and anti-inflammatory properties, were not modulated by ES (IL-6: *Ctrl:* 1.03 ± 0.11, *ES:* 1.17 ± 0.13, $t(10) = 0.857$, *ns*; TNFα: *Ctrl:* 1.01 ± 0.08, *ES:* 1.11 ± 0.08, $t(10) = 0.8489$, *ns*; IL-10: *Ctrl:* 1.12 ± 0.266, *ES:* 0.63 ± 0.199, $t(8) = 1.485$, *ns*). In addition, expression of microglial activation marker CD11b was not affected by ES exposure in P9 pups (*Ctrl:* 1.01 ± 0.08, *ES:* 0.96 ± 0.12, $t(10) = 0.691$, *ns*), while expression of CD68 tended to be decreased after ES, but this did not reach significance (*Ctrl:* 1.02 ± 0.09, *ES:* 0.64 ± 0.16, $t(10) = 2.092$, $p = 0.0629$).

3.3.3. Iba1 cell density is reduced in the EC after ES exposure

We questioned whether the influences of ES on microglial Iba1 are specific for the DG, or whether a similar impact of ES can be observed in other brain regions, like the EC. A similar analysis of microglial Iba1 immunostaining was performed in the EC (Fig. 3F) as described for the DG to address whether the impact of ES is specific for the hippocampus. Iba1 coverage as well as density of Iba1 cells in the EC was reduced in ES mice (Fig. 3G, H; Iba1 coverage: *Ctrl:* 14.72 ± 0.98, *ES:* 9.66 ± 0.52, $t(13) = 4.373$, $p < 0.001$; Iba1 cell density: *Ctrl:* 457.8 ± 13.01, *ES:* 340.10 ± 7.99, $t(13) = 7.433$, $p < 0.001$). Classification of the different morphological subtypes within the EC showed a tendency to a reduction in ramified cells after ES, but this and as well as the number of other morphological subtypes were not significantly altered (Fig. 3I; Ramified: *Ctrl:* 70.77 ± 6.80, *ES:* 46.97 ± 8.62, $t(9) = 2.099$, $p = 0.065$; Thick/long: *Ctrl:* 23.79 ± 5.38, *ES:* 36.26 ± 7.23, $t(9) = 1.335$, *ns*; Stout: *Ctrl:* 5.45 ± 2.04, *ES:* 14.79 ± 4.76, $t(9) = 1.676$, *ns*; Amoeboid: *Ctrl:* 0.0 ± 0.0, *ES:* 1.97 ± 1.36, $t(9) = 1.314$, *ns*).

Detailed analyzes of individual cells showed that ES does not alter the branching complexity or the cell size in the EC. Sholl analysis indicated that the complexity is not significantly different between Ctrl and ES Iba1 cells in the EC (Fig. 3J, condition F (1,5709) = 0.940, ns). Cellular surface of Iba1 cells, complexity of branching as well as soma diameter was not affected by ES, while the number of primary processes was significantly reduced by ES exposure (Cellular surface: *Ctrl:* 90.07 ± 11.89, *ES:* 87.24 ± 15.67, $t(10.949) = 0.734$, *ns*; Soma diameter: *Ctrl:* 7.44 ± 0.29, *ES:* 8.09 ± 0.34, $t(10.466) = 1.523$, *ns;* Primary process number: *Ctrl:* 4.34 ± 0.21, *ES:* 3.69 ± 0.17, $t(11.277) = 2.588$, $p = 0.025$).

3.4. ES affects the neuroinflammatory response in the hippocampus of WT and APP/PS1 mice at 4 months

3.4.1. ES and APP increase Iba1 immunoreactivity in the hippocampus

Iba1 immunopositive microglia were quantified at 4 months of age in WT as well as APP/PS1 mice for the same parameters as described for the P9 mice (see above) to assess if ES has lasting effects (Fig. 4A) and whether mild amyloid pathology affects microglia differentially in Ctrl vs. ES exposed mice. Iba1 cell density was increased in APP/PS1 mice while ES exposure only tends to increase the Iba1 cell density within the ML of the DG without reaching significance (Fig. 4B, *condition* $F(1,30) = 3.847$, $p = 0.059$, *genotype* $F(1,30) = 7.311$, $p = 0.011$, *interaction* $F(1,30) = 0.739$, *ns*). Also, coverage of Iba1 in the ML of the DG was not affected by ES in the WT mice but significantly increased in Ctrl APP/PS1 males compared to Ctrl WT. APP/PS1 overexpression however did not increase Iba1 coverage in mice with a history of ES exposure (*condition* $F(1,30) = 0.016$, *ns*, *genotype* $F(1,30) = 3.85$, $p = 0.059$, *interaction* $F(1,30) = 5.90$, $p = 0.021$*; post-hoc Ctrl WT vs Ctrl APP/PS1* $p = 0.030$). Similar to the ML of the DG, Iba1 cell density within the SLM and SR of the CA1 was significantly increased by ES exposure and APP/PS1 overexpression increased Iba1 coverage in this region (Fig. 4C; Iba1 cell density: *condition* $F(1,30) = 4.216$ $p = 0.049$, *genotype* $F(1,30) = 1.404$, *ns*, *interaction* $F(1,30) = 1.137$, ns; Iba1 coverage: *condition* $F(1,30) = 2.140$, *ns*, *genotype* $F(1,30) = 5.540$, $p = 0.026$, *interaction* $F(1,30) = 1.170$, *ns*). Analysis of Iba1 immunostaining in the EC (Supplementary Fig. 1A) showed no alteration in the density of Iba1 cells or Iba1 coverage within this region by ES or APP/PS1 (Supplementary Fig. 1B; Iba1 cell density: condition $F(1,33) = 2.389$, *ns*, *genotype* $F(1,33) = 0.074$, *ns*, *interaction* $F(1,33) = 1.114$, *ns*; Iba1 coverage: *condition* $F(1,32) = 1.392$, *ns*, *genotype* $F(1,32) = 0.749$, *ns*, *interaction* $F(1,32) = 0.204$, *ns*).

Microglial complexity as analyzed by Sholl analysis was not affected at 4 months by ES exposure or by amyloid overexpression (Fig. 4D *condition* $F(1,13029) = 0.62$, *ns*, *genotype* $F(1,13029) = 0.29$, *ns*, *interaction* $F(1,13029) = 0.23$, *ns*; primary branching: *condition* $F(1,11.970) = 0.155$, *ns*, *genotype* $F(1,11.971) = 0.170$, *ns*, *interaction* $F(1,12.107) = 0.268$, *ns*). Classification of these same microglia based on the morphological appearance was not affected by ES or APP/PS1 (Ramified: *condition* $F(1,20) = 0.198$, *ns*, *genotype F* $(1,20) = 3.235$, *ns*, *interaction* $F(1,20) = 3.058$, *ns*; Intermediate: *condition* $F(1,20) = 0.161$, *ns*, *genotype* $F(1,20) = 3.471$, *ns*, *interaction F* $(1,20) = 3.287$, *ns*, no amoeboid cells were present). Similarly, both microglial complexity, primary branching as well as classification of the morphological appearance were not altered by ES and APP/PS1 in the EC either (Supplementary Fig. 1C; Complexity: *condition* $F(1,12676) = 0.17$, *ns*, *genotype* $F(1,12676) = 0.94$, *ns*, *interaction* $F(1,12676) = 0.42$, *ns*; Primary branching: *condition F* $(1,22.930) = 2.379$, *ns*, *genotype* $F(1,22.821) = 1.518$, *ns*, *interaction* $F(1,23.311) = 1.830$, *ns*; Ramified: *condition* $F(1,20) = 0.120$, *ns*, *genotype* $F(1,20) = 2.447$, *ns*, *interaction* $F(1,20) = 0.058$, *ns*; Intermediate: *condition* $F(1,20) = 0.120$, *ns*, *genotype* $F(1,20) = 2.447$, *ns*, *interaction* $F(1,20) = 0.058$, *ns*; no amoeboid cells were present).

3.4.2. CD68 coverage is elevated in the hippocampus by ES and APP/PS1 at 4 months

CD68 immunoreactivity in the hippocampus was increased by ES exposure and by APP/PS1 overexpression. The APP/PS1 induced increase was further elevated in mice with a history of ES (Fig. 4E). In the DG and the CA, ES and APP/PS1 both significantly increased CD68 coverage (Fig. 4F, G; DG: *condition* $F(1,24) = 12.350$, $p = 0.002$, *genotype* $F(1,24) = 7.869$, $p = 0.010$, *interaction* $F(1,24) = 1.348$, *ns*; CA: *condition* $F(1,25) = 14.350$, $p = 0.001$, *genotype* $F(1,25) = 4.368$, $p = 0.047$, *interaction* $F(1,25) = 1.787$, *ns*). CD68 immunostaining in the EC (Supplementary Fig. 1D) was increased by APP/PS1, but not by previous ES exposure (Supplementary Fig. 1E; *condition* $F(1,28) = 3.097$, *ns*, *genotype* $F(1,28) = 13.680$, $p < 0.001$, *interaction* $F(1,28) = 0.931$, *ns*).

3.4.3. Expression of neuroinflammatory mediators in the hippocampus is affected by both ES and APP/PS1

When we analyzed hippocampal expression of CD11b and various cytokines, CD11b and IL-6 mRNA were differentially affected by ES in WT vs APP/PS1, however the *post-hoc* analysis did not reveal significance (Fig. 4H, I; CD11b: *condition* $F(1,18) = 0.355$, *ns*, *genotype* $F(1,18) = 0.239$, *ns*, *interaction* $F(1,18) = 8.464$, $p = 0.009$*; no significant post-hoc effects*; IL-6: *condition* $F(1,17) = 1.526$ *ns*, *genotype* $F(1,17) = 0.021$, *ns*, *interaction* $F(1,17) = 5.404$, $p = 0.033$*; no significant post-hoc effects*). Considering the strong interaction effects we analyzed how ES affects the expression in WT mice only and found that ES tended to increase CD11b expression and reduces IL-6 expression in WT mice (CD11b: *Ctrl WT:* 1.00 ± 0.06, *ES WT:* 1.18 ± 0.06, $t(10) = 2.107$, $p = 0.061$; IL6: *Ctrl WT:* 1.08 ± 0.16, *ES WT:* 0.52 ± 0.09, $t(9) = 2.746$, $p = 0.023$). Furthermore IL-1β mRNA expression was not affected by ES or APP/PS1 overexpression (Fig. 4J, *condition* $F(1,17) = 0.036$, *ns*, *genotype* $F(1,17) = 0.105$, *ns*, *interaction* $F(1,17) = 0.131$, *ns*) and TNFα mRNA expression was elevated by APP/PS1 overexpression but not differentially by ES (Fig. 4K, *condition* $F(1,17) = 0.002$, *ns*, *genotype* $F(1,17) = 6.148$, $p = 0.024$, *interaction* $F(1,17) = 0.004$, *ns*).

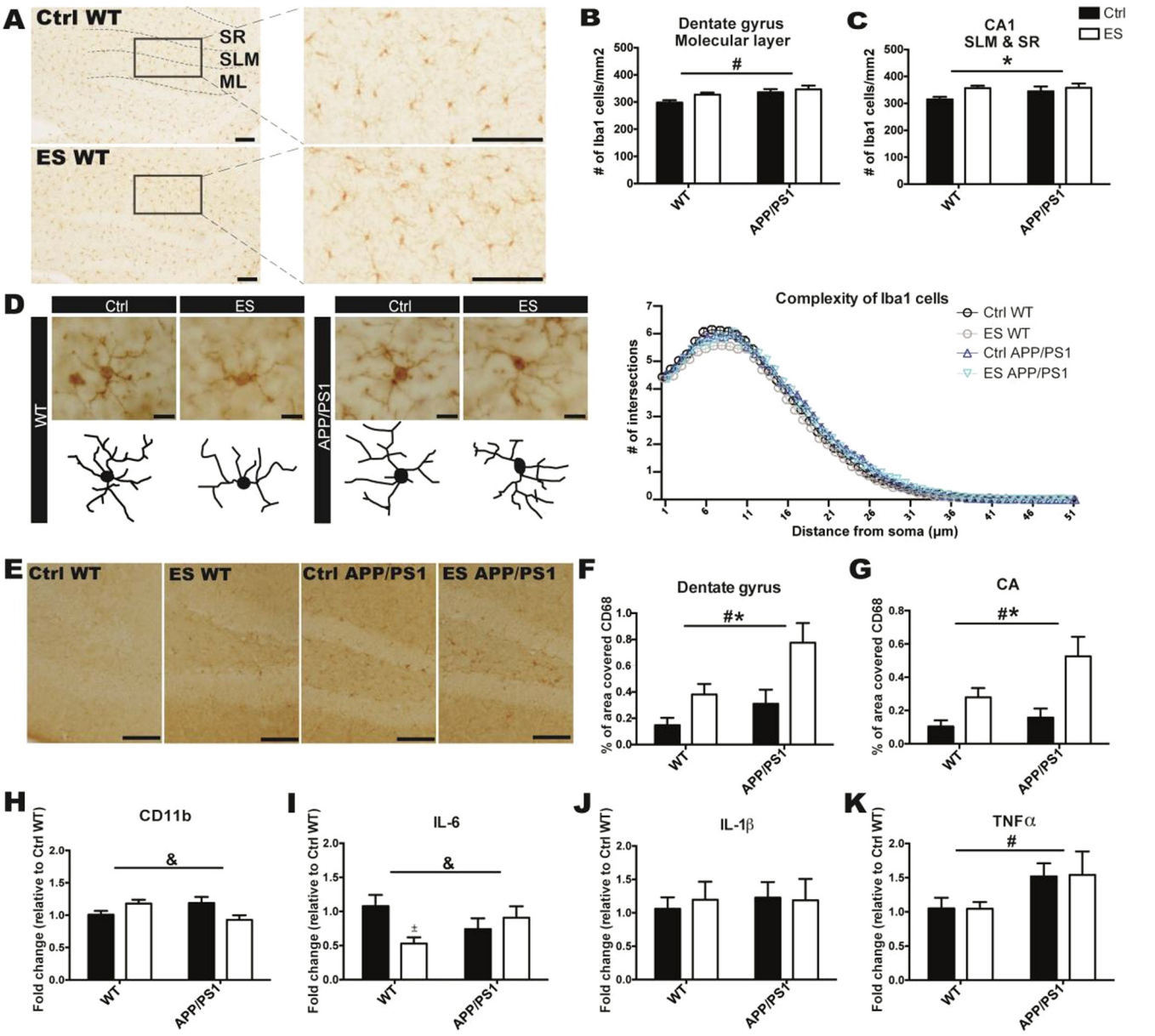

Fig. 4. ES modulates the neuroinflammatory response in adult WT and APP/PS1 mice at 4 months. A) Representative images of Iba1 immunoreactive cells in Ctrl WT and ES WT males at 4 months. Anatomical locations of the molecular layer (ML) of the dentate gyrus (DG), stratum lacunosum-moleculare (SLM) and stratum radiatum (SR) of the cornu ammonis (CA)1 are highlighted and presented in a higher magnification image. B) APP/PS1 overexpression increased Iba1 cell density in the ML of DG, while ES exposure tended to increase this as well. C) ES exposure increased Iba1 cell density in the SLM and SR of the CA1 without an effect of APP/PS1. D) Complexity of Iba1 cells is not affected by either ES or APP/PS1. E) Representative images of CD68 immunoreactive cells in 4 month old Ctrl WT, ES WT, Ctrl APP/PS1 and ES APP/PS1 males. F) CD68 coverage is increased in the DG by both ES and APP/PS1 overexpression. Similarly, G) CD68 coverage is increased in the CA by ES and APP/PS1 overexpression. H) Expression of CD11b and I) IL-6 are affected by a condition-genotype interaction, but no significant post-hoc effects could be determined. Still, a separate t-test indicates that ES reduced IL-6 expression in ES WT in comparison to Ctrl WT. J) IL-1β expression is not affected by ES or APP/PS1. K) TNFα is increased in APP/PS1 males. Black bars represent Ctrl groups, white bars ES groups. Scale bar: A,E) 100 µm, D) 10 µm. *: condition effect, #: genotype effect, &: interaction effect. Separate *t*-test: ±: sig from Ctrl WT.

3.5. Microglial activation in response to amyloid pathology at an advanced pathological stage is reduced by ES exposure

3.5.1. Microglial activation in APP/PS1 mice in the hippocampus is reduced after ES

Iba1 immunoreactive microglia in the brains of 10 month old mice, in addition to containing individual Iba1 immunoreactive cells, also showed a clustering of Iba1 cells in APP/PS1 mice at this advanced pathological age in both the hippocampus (Fig. 5A) and in the EC (Supplementary Fig. 2A). Therefore, we quantified next to Iba1 coverage, cell density and complexity of individual Iba1 cells also coverage of clustered Iba1. In addition, we analyzed the ratio of Iba1 coverage/plaque load, to gain further insight into the association between Iba1 activation and plaque accumulation. There was an increase in Iba1 coverage in the DG and CA1 of Ctrl APP/PS1 mice when compared to Ctrl WT mice, which was reduced after ES exposure (Fig. 5B, C; DG ML: *condition* $F(1,23) = 7.327$, $p = 0.013$, *genotype* $F(1,23) = 55.774$, $p < 0.001$, *interaction* $F(1,23) = 1.427$, $p = 0.024$; CA1 SML & SR: *condition* $F(1,23) = 4.270$, $p = 0.050$, *genotype* $F(1,23) = 26.492$, $p < 0.001$, *interaction* $F(1,23) = 0.172$, $p = 0.839$). Furthermore, APP/PS1 overexpression significantly increased Iba1 cell density of individual Iba1 cells in the ML of the DG, but not in CA1, and ES did not affect this further (DG ML: *condition* $F(1,23) = 2.460$, *ns*, *genotype* $F(1,23) = 12.840$,

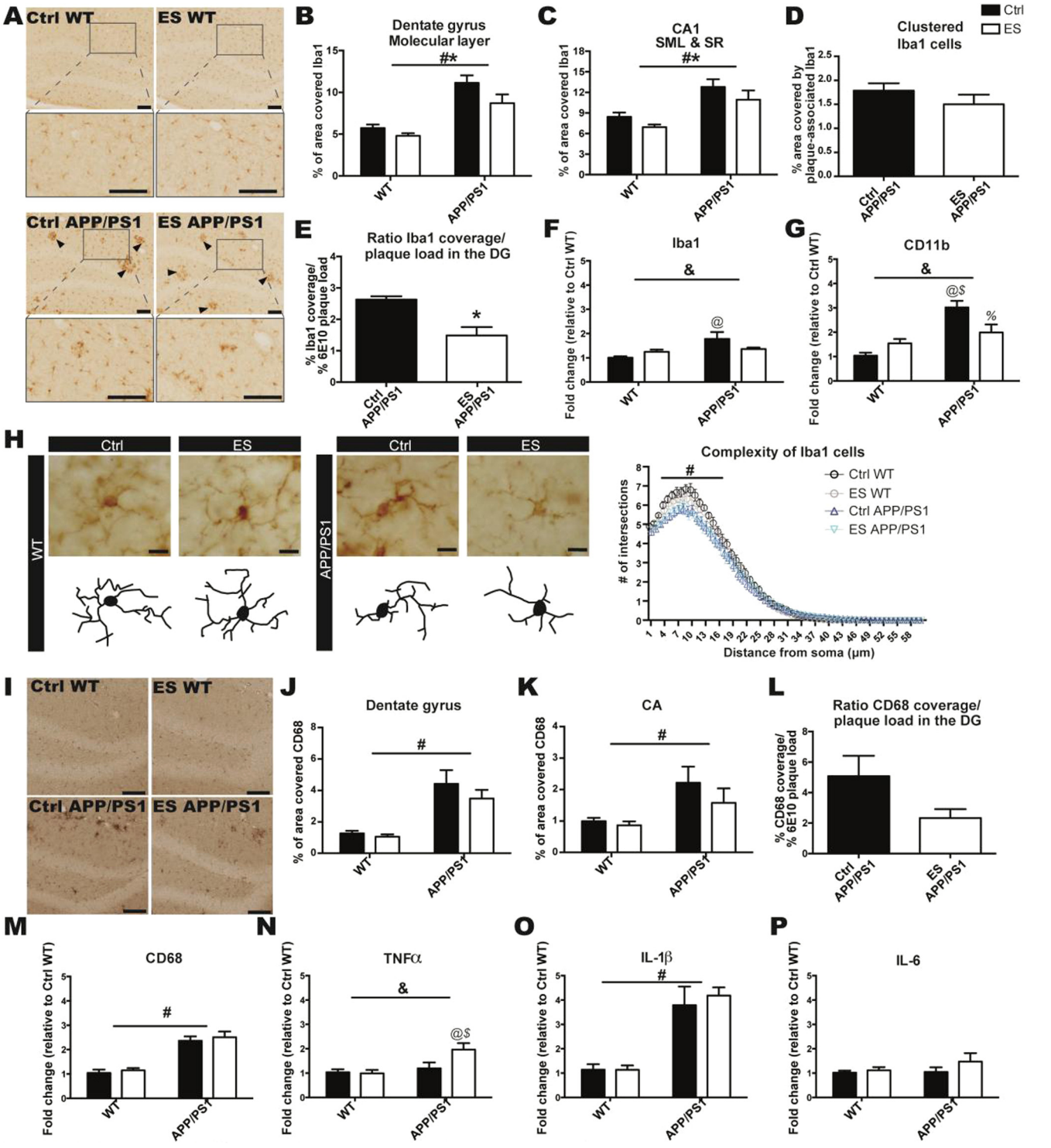

Fig. 5. ES exposed APP/PS1 mice show less prominent microglial activation. A) Representative images of Iba1 immunostaining in the DG of 10 month old WT and APP/PS1 animals exposed to Ctrl or ES. Arrowheads point to clustering of Iba1 cells related to amyloid in APP/PS1 mice. The magnified image specifically represents Iba1 in the molecular layers of the DG and CA. B) In the molecular layer of the DG and C) the CA1 SLM & SR the coverage of Iba1 immunostaining is significantly increased in APP/PS1 animals, but decreased in ES animals. D) Separate analysis of Iba1 clustering shows that ES does not increase Iba1 clustering related to plaque pathology in the DG of APP/PS1 animals, while E) the ratio clustered Iba1 coverage/ plaque load is reduced after ES. F) Expression of Iba1 mRNA is increased in Ctrl APP/PS1 mice in comparison to Ctrl WT, while Iba1 expression in ES APP/PS1 is not elevated. G) Similarly to Iba1 mRNA expression, CD11b expression is significantly increased in Ctrl APP/PS1 in comparison to WT mice, but to a lesser extent in ES APP/PS1 mice. H) The tracing of hilar Iba1 cells indicates an overall decrease in the complexity of microglia in APP/PS1 animals, specifically at 3 µm to 17 µm from the soma. I) CD68 immunostaining in the DG of 10 month old mice shows that J, K) CD68 coverage is elevated in APP/PS1 mice in comparison to WT in both the DG and CA, without an effect of ES exposure. L) The ratio of clustered CD68 coverage/ plaque load does not differ between Ctrl and ES APP/PS1. M) Expression of CD68 mRNA is elevated by APP/PS1, but ES does not affect this expression. N) Expression of TNFα is significantly increased in ES APP/PS1 in comparison to Ctrl WT and ES WT and O) IL-1β expression is elevated in both Ctrl and ES exposed APP/PS1 mice. P) Expression of IL-6 is not significantly affected by both ES and APP/PS1. Black bars represent Ctrl groups, white bars ES groups. Scale bar: A,I) 100 µm, H) 10 µm. *: condition effect, #: genotype effect, &: interaction effect. Post-hoc annotations: @: sig from Ctrl WT; $: sig from ES WT, *: sig from Ctrl APP/PS1.

$p = 0.002$, *interaction* $F(1,23) = 0.004$, *ns*; CA1 SML & SR: *condition* $F(1,23) = 1.822$, *ns, genotype* $F(1,23) = 0.797$, *ns, interaction* $F(1,23) = 0.001$, *ns*). Iba1 coverage and cell density in the EC were similarly increased in APP/PS1 mice, irrespective of previous ES exposure (Supplementary Fig. 2B; Coverage: *condition* $F(1,23) = 0.034$, *ns, genotype* $F(1,23) = 42.337$, $p < 0.001$, *interaction* $F(1,23) = 0.016$, *ns*; Cell density: *condition* $F(1,23) = 0.739$, *ns, genotype* $F(1,23) = 11.496$, $p = 0.003$, *interaction* $F(1,23) = 0.191$, *ns*). Coverage of clustered Iba1 in the DG, present only in the APP/PS1 mice, was not affected by ES exposure (Fig. 5D, *Ctrl:* 1.79 ± 0.28, *ES:* 1.50 ± 0.40, $t(8) = 1.144$, *ns*). Interestingly, however, the ratio Iba1 coverage/-plaque load is significantly reduced by 43.4% in the ES exposed APP/PS1 mice (Fig. 5E, *Ctrl:* 2.63 ± 0.11, *ES:* 1.49 ± 0.26, $t(7) = 4.367$, $p = 0.003$), whereas in the EC both the coverage of clustered Iba1 and the ratio Iba1 coverage/plaque load is not affected by ES (Supplementary Fig. 2C, D; coverage clustered Iba1: *Ctrl:* 18.42 ± 1.23, *ES:* 16.84 ± 2.32, $t(8) = 0.660$, *ns*; ratio coverage Iba1/-plaque load: *Ctrl:* 1.60 ± 0.34, *ES:* 1.03 ± 0.14, $t(8) = 1.320$, *ns*). Similarly, Iba1 and CD11b mRNA expression was elevated in APP/PS1 compared to WT mice under control conditions, and this elevation was not, or less strongly, present in the APP/PS1 mice exposed to ES (Fig. 5F, G; Iba1 mRNA expression: *condition* $F(1,22) = 0.354$, *ns, genotype* $F(1,22) = 8.540$, $p = 0.008$, *interaction* $F(1,22) = 4.750$, $p = 0.040$; *post-hoc Ctrl WT vs Ctrl APP/PS1* $p = 0.011$; CD11b mRNA expression: *condition* $F(1,23) = 1.280$, *ns, genotype* $F(1,23) = 27.300$, $p < 0.001$, *interaction* $F(1,23) = 11.000$, $p = 0.003$; *post hoc Ctrl WT vs Ctrl APP/PS1* $p < 0.001$, *ES WT vs Ctrl APP/PS1* $p < 0.001$, *Ctrl APP/PS1 vs ES APP/PS1* $p = 0.038$).

Next to Iba1 coverage and cell density, effects of ES and APP/PS1 on the complexity and morphology-based classification of individual microglia were quantified. Microglia of APP/PS1 mice show reduced complexity of Iba1 cells in both the DG and EC, when compared to WT without an effect of previous ES exposure (Fig. 5H, Supplementary Fig. 2E; DG: *condition* $F(1,13310) = 0.59$, *ns, genotype* $F(1,13310) = 4.87$, $p = 0.027$, *interaction* $F(1,13310) = 0.75$, *ns*; EC: *condition* $F(1,12278) = 1.02$, *ns, genotype* $F(1,12278) = 6.34$, $p = 0.012$, *interaction* $F(1,12278) = 0.41$, *ns; post-hoc: APP/PS1 significant lower than WT at* 1 μm *to* 17 μm *from the soma*). No differences were, however, present in the classification of these same cells based on their morphology in the hippocampus (Ramified: *condition* $F(1,18) = 2.175$, $p = ns$, *genotype* $F(1,18) = 1.988$, $p = ns$, *interaction* $F(1,18) = 1.131$, $p = 0.302$; Intermediate: *condition* $F(1,18) = 1.734$, $p = ns$, *genotype* $F(1,18) = 0.348$, $p = ns$, *interaction* $F(1,18) = 1.313$, $p = ns$; Amoeboid: *condition* $F(1,18) = 3.379$, $p = ns$, *genotype* $F(1,18) = 3.379$, $p = ns$, *interaction* $F(1,18) = 3.379$, $p = ns$). APP/PS1 shifted the morphological appearance of Iba1 cells in the EC of about 10% of the cells from ramified to more intermediate or amoeboid, independent of previous ES exposure (Ramified: *condition* $F(1,18) = 0.726$, *ns, genotype* $F(1,18) = 18.362$, $p < 0.001$, *interaction* $F(1,18) = 2.191$, *ns*; Intermediate: *condition* $F(1,18) = 0.879$, *ns, genotype* $F(1,18) = 15.582$, $p < 0.001$, *interaction* $F(1,18) = 2.496$, *ns*; Amoeboid: *condition* $F(1,18) = 0.088$, *ns, genotype* $F(1,18) = 3.847$, $p = 0.065$, *interaction* $F(1,18) = 0.088$, *ns*).

3.5.2. Microglial CD68 is enhanced in APP/PS1 mice and not affected by ES exposure at 10 months

Immunostaining for CD68 revealed abundant CD68 immunoreactive cells in the DG of 10 month old mice, and clustered CD68 immunoreactive cells in APP/PS1 mice (Fig. 5I). In APP/PS1 mice, enhanced microglial CD68 coverage was found in the DG and CA without an effect of previous ES exposure in either WT or APP/PS1 mice (Fig. 5J, K; DG: *condition* $F(1,18) = 1.472$, *ns, genotype* $F(1,18) = 35.130$, $p < 0.001$, *interaction* $F(1,18) = 0.598$, *ns*; CA: *condition* $F(1,18) = 1.684$, *ns; genotype* $F(1,18) = 10.490$, $p = 0.005$, *interaction* $F(1,18) = 0.736$, *ns*). In APP/PS1 mice, ES did not significantly affect the ratio of clustered CD68 coverage/ plaque load (Fig. 5L, *Ctrl:* 5.08 ± 1.33, *ES:* 2.33 ± 0.59, $t(6) = 1.50$, *ns*). Furthermore CD68 mRNA expression was elevated by APP/PS1 overexpression, but not by previous ES exposure (Fig. 5M, *condition* $F(1,21) = 0.672$, *ns, genotype* $F(1,21) = 75.590$, $p < 0.001$, *interaction* $F(1,21) = 0.013$, *ns*). Similarly, the coverage of CD68 in the EC (Supplementary Fig. 2F) is increased in APP/PS1 mice, without an effect of ES (Supplementary Fig. 2G; *condition* $F(1,21) = 1.754$, *ns, genotype* $F(1,21) = 39.019$, $p < 0.001$, *interaction* $F(1,21) = 2.660$, *ns*). In addition, ES did not significantly affect the ratio of clustered CD68 coverage/ plaque load within the EC (Supplementary Fig. 2H; *Ctrl:* 1.42 ± 0.34, *ES:* 0.72 ± 0.36, $t(7) = 1.254$, *ns*).

3.5.3. Expression of neuroinflammatory mediators in the hippocampus is altered after ES in APP/PS1 at 10 months

The expression of TNFα mRNA, while not affected in Ctrl APP/PS1, was increased in ES APP/PS1 compared to WT mice (Fig. 5N, condition $F(1,25) = 3.530$, $p = 0.072$, genotype $F(1,25) = 8.760$, $p = 0.007$, interaction $F(1,25) = 4.470$, $p = 0.045$; *post-hoc* Ctrl WT vs ES APP/PS1 $p = 0.021$, ES WT vs ES APP/PS1 $p = 0.005$). In APP/PS1 mice, expression of the pro-inflammatory cytokine IL-1β was increased in both Ctrl and ES mice. IL-6 mRNA expression was not affected by either APP/PS1 of ES exposure (Fig. 5O, P; IL-1β: condition $F(1,25) = 0.250$, ns, genotype $F(1,25) = 53.140$, $p < 0.001$, interaction $F(1,25) = 0.260$ ns; IL-6: condition $F(1,25) = 1.695$, ns, genotype $F(1,25) = 0.937$, ns, interaction $F(1,25) = 0.689$,*ns*).

4. Discussion

We set out to test whether exposure to ES could affect amyloid pathology, modulate the neuroinflammatory profile, and alter the neuroinflammatory response to Aβ neuropathology in APP/PS1 mice at two different ages. Our results show that exposure to postnatal chronic ES: 1) had an age dependent and brain region specific effect on Aβ neuropathology. At 4 months of age, ES attenuated the cell-associated amyloid, while it aggravated Aβ plaque deposition at 10 months of age in the DG, without affecting EC neuropathology; 2) altered neuroinflammatory-related factors in WT mice, affecting different aspects directly after ES at P9 and at 4 months of age, without effects at 10 months of age; 3) modulated the neuroinflammatory response to Aβ pathology in APP/PS1 mice differently depending on the pathological stage. ES exposure increased the density of microglial Iba1 and phagocytic marker CD68 immunoreactivity at 4 months of age, when cell-associated amyloid was reduced by ES. In contrast, ES reduced microglial accumulation at the site of Aβ plaques at 10 months, which were increased by ES at this age. Overall, these effects appear more prominent in the hippocampus, whereas the EC showed no significant alterations upon ES in adult mice. Taken together, a brief exposure to chronic stress in the first week of life has pervasive effects on later-life Aβ pathology, on the neuroinflammatory response of WT mice, and on the response to Aβ accumulation in APP/PS1 mice.

4.1. Amyloid pathology in the hippocampus is affected by early-life stress in a pathological stage-dependent manner

The hippocampus of Ctrl APP/PS1 mice exhibited abundant cell-associated amyloid at 4 months of age, while Aβ plaques are sparse at this time. The level of cell-associated amyloid decreased with advancing age, whereas Aβ plaque load increased strongly in the DG and EC. This is a common feature in multiple APP transgenic mouse models (Christensen et al., 2009; Cuello, 2005; Ferretti et al., 2012; Garcia-Alloza et al., 2006; LaFerla et al., 2007; Yu et al., 2009). ES further modulated the pathology in the DG, depending on the age, hence the pathological stage. To the best of our knowledge, we describe here for the first time, that chronic

ES appears protective at an early pathological stage, but has deleterious effects when pathology progressed in later life. In fact, even though only few Aβ plaques have developed in non-stressed APP/PS1 mice at 4 months of age, ES lowered cell-associated amyloid suggesting a reduction in Aβ production, or an increased clearance, which may cause an initial delay in Aβ neuropathology by ES. This is in contrast to the elevation in Aβ plaque pathology in middle-aged ES APP/PS1 mice. Such aggravation of the neuropathology at an advanced pathological stage is in line with other effects described after chronic ES (Lesuis et al., 2016; Sierksma et al., 2012) and after exposure to chronic stress at an adult age (Jeong, 2006). Also, the observed alterations after ES in this study only appeared in the hippocampus, rather than the EC. We can only speculate why the hippocampus is more susceptible to a modulation by ES at 4 and 10 months, for instance due to the difference in pathological stage at these ages (Jankowsky et al., 2004), or a higher susceptibility of the hippocampus for perturbation upon stress exposure during early-life (Lucassen et al., 2013).

When considering possible mediators of the ES effects on Aβ accumulation, glucocorticoids are an obvious candidate. Indeed, there is considerable evidence that glucocorticoids in adult rats (Catania et al., 2009) and in triple-transgenic (3xTG) mice (Green et al., 2006) steer APP processing towards an amyloidogenic pathway. However, in the current study a direct effect of glucocorticoid exposure seems less plausible as ES exposure (i.e. elevation in corticosterone; Naninck et al., 2015) occurs several months before Aβ accumulation becomes detectable, and is aggravated by ES. This suggests that instead of direct effects of corticosterone, ES is likely to have programmed systems involved in Aβ clearance, production and/or deposition. Interestingly, a large body of literature supports an essential role for inflammatory changes and microglia in response to Aβ accumulation and Aβ clearance (Fu et al., 2012; Liu et al., 2010; Majumdar et al., 2007; Wang et al., 2016). We therefore hypothesized that ES might (re-)program neuroinflammatory properties that could affect the response to the gradual age-dependent buildup of Aβ thereby influencing the subsequent progression of AD pathology.

4.2. ES affects the hippocampal neuroinflammatory response in P9 and adult wild-type mice

Microglia change their transcriptional profile and morphological appearance during different stages of development (Alliot et al., 1999; Matcovitch-Natan et al., 2016; Schwarz et al., 2012), and morphology of microglia therefore provides a good reflection of their maturity and activational status (Schwarz et al., 2012). Microglia of Ctrl WT mice at P9 exhibited an intermediate, not yet fully ramified morphology, suggesting an immature state, similar to that described for rats at P4 (Schwarz et al., 2012). Exposure to ES reduced the coverage of Iba1 immunoreactive cells in both the DG and EC. Although the reduced coverage resulted from less microglial complexity in the DG, it was due to reduced microglial cell density in the EC. The altered microglia coverage in ES mice at P9 is further accompanied by elevated mRNA expression of pro-inflammatory cytokine IL-1β in the hippocampus, in line with the aberrant cytokine expression profile following other ES paradigms (do Prado et al., 2015; Roque et al., 2016).

Interestingly, chronic ES-induced effects observed in our mice differ slightly from those in previous studies of other ES paradigms (Delpech et al., 2016; Gómez-González and Escobar, 2009; Roque et al., 2016; Roque et al., 2014; Ślusarczyk et al., 2015). These differences might be attributed to the different periods during which ES exposure occurs. The developmental stage during ES exposure likely determines the (differential) vulnerability of microglia for perturbations by stress, depending on the changes in their transcriptional profile and activational status during development (Matcovitch-Natan et al., 2016; Schwarz et al., 2012). The regional differences in ES-induced effects on microglia within the DG and EC might similarly reflect a different developmental stage of these two regions during stress exposure; the EC is already largely developed by P2, whereas the DG still undergoes mayor developmental changes during the first two postnatal weeks (Altman and Bayer, 1990; Bayer, 1980).

Overall, the perinatal stress-induced alterations in the neuroinflammatory profile during early hippocampal development, and elevated IL-1β specifically, can be detrimental for proper brain development (Allan et al., 2005; Felderhoff-Mueser et al., 2005; Vela, 2002). Such alterations might also lead to an altered neuroinflammatory profile and responsiveness in later-life. Indeed, postnatal ES exposure elevated Iba1 cell density and the phagocytic marker CD68 in the hippocampus of 4 month old ES WT mice, accompanied by reduced IL-6 mRNA expression. Interestingly, phagocytic activity in maternally separated mice was similarly increased at 4 weeks of age (Delpech et al., 2016), however these animals were not followed up to adulthood. The ES-induced effects on Iba1 and CD68 in WT mice are, however, normalized by 10 months of age. The transient character of the increase in Iba1 cell density might be explained by a temporal overshoot in proliferation during the first few weeks after ES exposure, as the microglial population expands rapidly during that period (Alliot et al., 1999; Reemst et al., 2016).

Altogether, ES clearly affects neuroinflammatory aspects at P9 as well as in adulthood. The question remains whether these alterations in microglia have consequences for hippocampal functioning as well. It is interesting to speculate for instance if these changes might contribute to the reductions in hippocampal neuronal plasticity found after chronic ES, i.e. neurogenesis, spine pruning and reductions found in synaptic connectivity (Naninck et al., 2015; Liu et al., 2016; Wang et al., 2013). It is furthermore important to understand how such alterations affect the responsiveness of microglia to a subsequent challenge, thereby potentially contributing to a more vulnerable phenotype.

4.3. Previous ES exposure alters the microglial response in APP/PS1 and might contribute to alterations in Aβ pathology

Accumulation of Aβ triggered a neuroinflammatory response in APP/PS1 mice confirming and extending findings by others (Babcock et al., 2015; Baron et al., 2014; Guo et al., 2015; Zhang et al., 2012). This neuroinflammatory phenotype is further modulated by ES exposure. It is intriguing that the ES-induced reduction in cell-associated amyloid at an early pathological stage (4 months), was accompanied by enhanced CD68 in the hippocampus. This might suggest that ES exposure has a protective effect in APP/PS1 mice at this early pathological stage through elevated internalization and/or phagocytosis of pre-plaque Aβ peptides. On the other hand, at a more advanced pathological stage, ES rather aggravated the plaque pathology in 10 month old ES APP/PS1 mice, accompanied by reduced microglial accumulation, and a potentiated increase in pro-inflammatory TNFα. Our data thus suggest that ES affects microglial responses to Aβ in an age- or pathological stage-dependent fashion, which may contribute to the progression of Aβ pathology in APP/PS1 mice.

The observed differences between WT and APP/PS1 mice highlight the importance of the early-life environment for later-life neuroinflammatory responsiveness to specific stimuli. Middle-aged WT mice exposed to ES do not seem different from Ctrl WT mice in terms of the neuroinflammatory profile at 10 months of age. However, a challenging environment or inflammatory insult that stimulates the neuroinflammatory response in ES mice, such as Aβ accumulation in APP/PS1 mice, can reveal lasting consequences of ES for microglial functioning. Our findings thus suggest

that ES programs or sensitizes microglia that thereby respond differently upon later challenges or stimulati. Such sensitization is in line with prenatal ES studies showing an exacerbated pro-inflammatory release of microglia in response to LPS (Diz-Chaves et al., 2013; Szczesny et al., 2014). However, whether such an acute response to LPS after ES is mediated through the same sensitization or programming mechanisms as the response to chronic Aβ accumulation in APP/PS1 mice remains to be determined.

It is important to note that the markers Iba1, CD11b and CD68, that are typically used to label endogenous microglia, are also expressed by perivascular macrophages and infiltrating myeloid cells originating from the bone-marrow, which can infiltrate the brain under pathological conditions (Greter et al., 2015; Prinz and Priller, 2014; Prinz et al., 2011). Although there is, to our knowledge, no evidence for altered infiltration of peripheral cells upon experiences of ES or stress in general, there is evidence both supporting (Mildner et al., 2011; Simard et al., 2006) and opposing (Meyer-Luehmann and Prinz, 2015) contributions of myeloid cells in relation to Aβ clearance in the AD brain. Future studies are therefore needed to elucidate whether infiltration of peripheral cells might contribute to the observed phenotype in ES APP/PS1.

One of the open questions is whether or not alterations in Aβ neuropathology and neuroinflammation correlate with cognitive functioning throughout life. Previous studies describe how the currently employed chronic ES models leads to cognitive impairments at 4 months of age (Naninck et al., 2015; Rice et al., 2008), whereas APP/PS1 mice typically exhibit impairments in various spatial memory tasks only after ±6 months of age (Han et al., 2016; Puoliväli et al., 2002; Trinchese et al., 2004; Zhang et al., 2011), although in several AD mouse models, there is evidence for a lack of correlation between alterations in Aβ plaque levels and behavioral outcome (Baglietto-Vargas et al., 2015; Giménez-Llort et al., 2007; Jaworski et al., 2010; Marlatt et al., 2013). Clearly at this point we can only speculate, but it is possible that the ES-induced amelioration in amyloid pathology at 4 months of age might also delay the onset of cognitive impairments in APP/PS1 mice. Considering the elevation in Aβ plaque load in the DG of ES APP/PS1 mice at 10 months, this would then be expected to aggravate cognitive impairments at this age. This would be in line with previous studies on effects of adult stress in APP mouse models (Han et al., 2016; Huang et al., 2015; Jeong, 2006).

4.4. Conclusion

We demonstrate that ES impacts microglia throughout life, as summarized in Fig. 6 as a graphical abstract. The altered neuroinflammatory response can potentially contribute to the consequences of ES for brain development and later-life functions. Next, ES alters the microglial response to Aβ neuropathology in the APP/PS1 AD model. Changes in microglia and the neuroinflammatory response may contribute to these alterations, either by altered Aβ sensing or by developing a dysfunctional state. Thus,

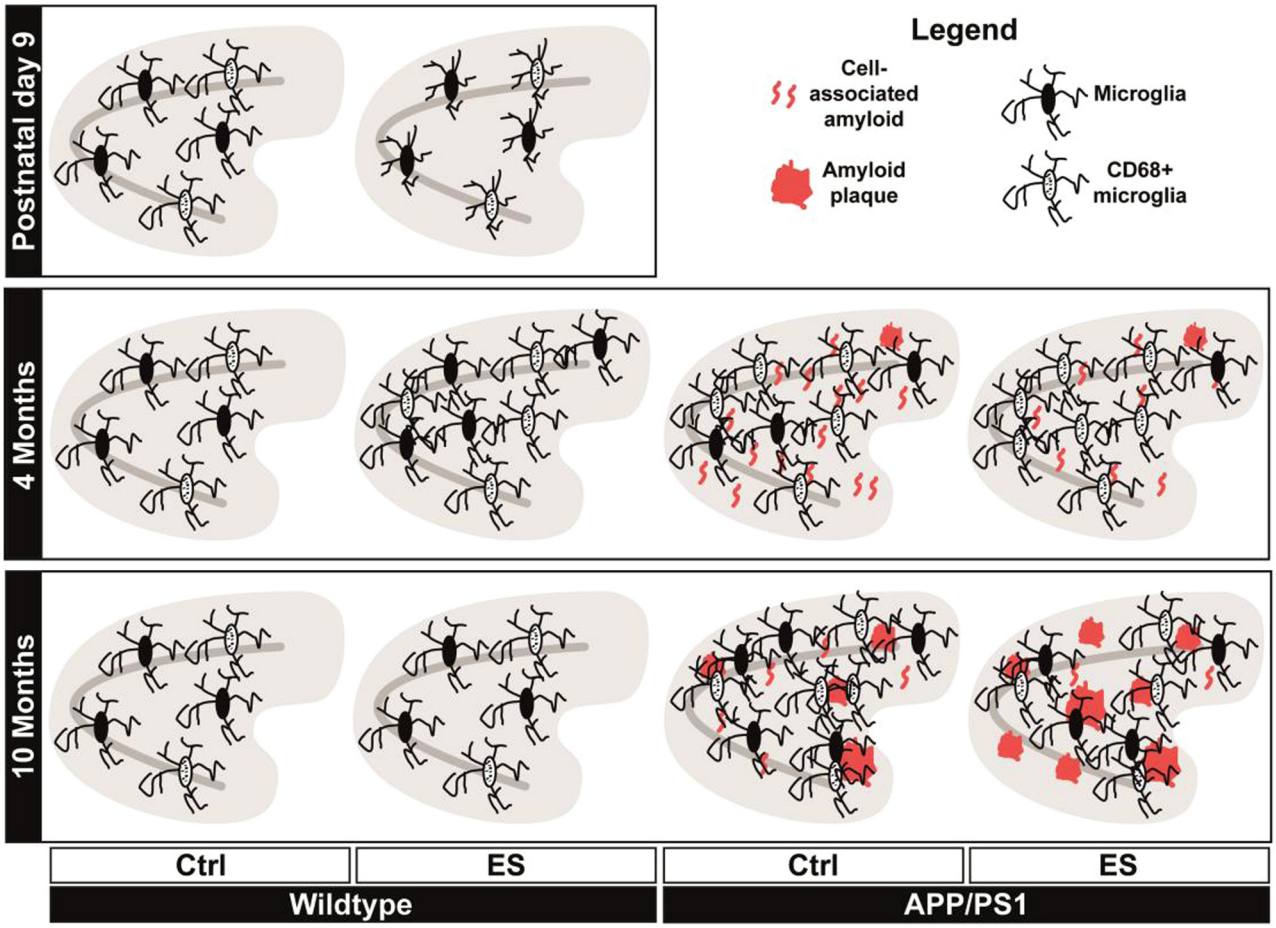

Fig. 6. Summarizing figure; stress exposure during early-life has immediate and lasting effects on microglia in the hippocampus. Directly after early-life stress (ES) exposure at postnatal day (P)9, the coverage of microglial Iba1 in the dentate gyrus of the hippocampus is reduced due to less complex cells. When these animals are followed up into young adulthood (4 months), ES induces a minor increase in microglial Iba1 cell numbers, which is accompanied by elevated coverage of microglial CD68. These effects in wild-type (WT) ES exposed mice at 4 months are, however, normalized when the mice reach middle-age (10 months). In APP/PS1 mice with continuously accumulating Aβ deposition, ES reduces cell-associated amyloid at 4 months, whereas again microglial CD68 and Iba1 cell density are increased at this age. Interestingly, when Aβ neuropathology has reached a progressed stage in 10 month old APP/PS1 mice, ES aggravated this neuropathology and reduced the microglial response.

even though ES experiences occur long before the accumulation of Aβ plaque depositions itself, a history of ES can have a lasting impact on the brain and potentially modify the progression of AD neuropathology.

Acknowledgments and funding

We thank Dr. Bart J.A. Pollux for his statistical support and help. LH, AK and PJL are supported by ISAO/Alzheimer Nederland, PJL is further supported by NWO PRIOMED and the HersenStichting Nederland.

Appendix A. Supplementary data

Supplementary data associated with this article can be found, in the online version, at http://dx.doi.org/10.1016/j.bbi.2016.12.023.

References

Allan, S.M., Tyrrell, P.J., Rothwell, N.J., 2005. Interleukin-1 and neuronal injury. Nat. Rev. Immunol. 5, 629–640. http://dx.doi.org/10.1038/nri1664.

Alliot, F., Godin, I., Pessac, B., 1999. Microglia derive from progenitors, originating from the yolk sac, and which proliferate in the brain. Brain Res. Dev. Brain Res. 117, 145–152.

Altman, J., Bayer, S.A., 1990. Migration and distribution of two populations of hippocampal granule cell precursors during the perinatal and postnatal periods. J. Comp. Neurol. 301, 365–381. http://dx.doi.org/10.1002/cne.903010304.

Babcock, A.A., Ilkjær, L., Clausen, B.H., Villadsen, B., Dissing-Olesen, L., Bendixen, A.T. M., Lyck, L., Lambertsen, K.L., Finsen, B., 2015. Cytokine-producing microglia have an altered beta-amyloid load in aged APP/PS1 Tg mice. Brain Behav. Immun. 48, 86–101. http://dx.doi.org/10.1016/j.bbi.2015.03.006.

Baglietto-Vargas, D., Chen, Y., Suh, D., Ager, R.R., Rodriguez-Ortiz, C.J., Medeiros, R., Myczek, K., Green, K.N., Baram, T.Z., LaFerla, F.M., 2015. Short-term modern life-like stress exacerbates Aβ-pathology and synapse loss in 3xTg-AD mice. J. Neurochem. 134, 915–926. http://dx.doi.org/10.1111/jnc.13195.

Bayer, S.A., 1980. Development of the hippocampal region in the rat II. Morphogenesis during embryonic and early postnatal life. J. Comp. Neurol. 190, 115–134. http://dx.doi.org/10.1002/cne.901900108.

Baron, R., Babcock, A.A., Nemirovsky, A., Finsen, B., Monsonego, A., 2014. Accelerated microglial pathology is associated with Aβ plaques in mouse models of Alzheimer's disease. Aging Cell 13, 584–595. http://dx.doi.org/10.1111/acel.12210.

Baumeister, D., Akhtar, R., Ciufolini, S., Pariante, C.M., Mondelli, V., 2015. Childhood trauma and adulthood inflammation: a meta-analysis of peripheral C-reactive protein, interleukin-6 and tumour necrosis factor-α. Mol. Psychiatry 21, 642–649. http://dx.doi.org/10.1038/mp.2015.67.

Beynon, S.B., Walker, F.R., 2012. Microglial activation in the injured and healthy brain: what are we really talking about? Practical and theoretical issues associated with the measurement of changes in microglial morphology. Neuroscience 225, 162–171. http://dx.doi.org/10.1016/j.neuroscience.2012.07.029.

Bilbo, S.D., Schwarz, J.M., 2012. The immune system and developmental programming of brain and behavior. Front. Neuroendocrinol. 33, 267–286. http://dx.doi.org/10.1016/j.yfrne.2012.08.006.

Bücker, J., Fries, G.R., Kapczinski, F., Post, R.M., Yatham, L.N., Vianna, P., Bogo Chies, J. A., Gama, C.S., Magalhães, P.V., Aguiar, B.W., Pfaffenseller, B., Kauer-Sant'Anna, M., 2015. Brain-derived neurotrophic factor and inflammatory markers in school-aged children with early trauma. Acta Psychiatr. Scand. 131, 360–368. http://dx.doi.org/10.1111/acps.12358.

Catania, C., Sotiropoulos, I., Silva, R., Onofri, C., Breen, K.C., Sousa, N., Almeida, O.F.X., 2009. The amyloidogenic potential and behavioral correlates of stress. Mol. Psychiatry 14, 95–105. http://dx.doi.org/10.1038/sj.mp.4002101.

Chomczynski, P., Sacchi, N., 2006. The single-step method of RNA isolation by acid guanidinium thiocyanate-phenol-chloroform extraction: twenty-something years on. Nat. Protoc. 1, 581–585. http://dx.doi.org/10.1038/nprot.2006.83.

Christensen, D.Z., Bayer, T.A., Wirths, O., 2009. Formic acid is essential for immunohistochemical detection of aggregated intraneuronal Abeta peptides in mouse models of Alzheimer's disease. Brain Res. 1301, 116–125. http://dx.doi.org/10.1016/j.brainres.2009.09.014.

Christensen, D.Z., Schneider-Axmann, T., Lucassen, P.J., Bayer, T.A., Wirths, O., 2010. Accumulation of intraneuronal Aβ correlates with ApoE4 genotype. Acta Neuropathol. 119, 555–566. http://dx.doi.org/10.1007/s00401-010-0666-1.

Chugani, H.T., Behen, M.E., Muzik, O., Juhász, C., Nagy, F., Chugani, D.C., 2001. Local brain functional activity following early deprivation: a study of postinstitutionalized Romanian orphans. NeuroImage 14, 1290–1301. http://dx.doi.org/10.1006/nimg.2001.0917.

Coelho, R., Viola, T.W., Walss-Bass, C., Brietzke, E., Grassi-Oliveira, R., 2014. Childhood maltreatment and inflammatory markers: a systematic review. Acta Psychiatr. Scand. 129, 180–192. http://dx.doi.org/10.1111/acps.12217.

Cuello, A.C., 2005. Intracellular and extracellular Abeta, a tale of two neuropathologies. Brain Pathol. 15, 66–71. http://dx.doi.org/10.1111/j.1750-3639.2005.tb00101.x.

Cunningham, C., 2013. Microglia and neurodegeneration: the role of systemic inflammation. Glia 61, 71–90. http://dx.doi.org/10.1002/glia.22350.

Delpech, J.-C., Wei, L., Hao, J., Yu, X., Madore, C., Butovsky, O., Kaffman, A., 2016. Early life stress perturbs the maturation of microglia in the developing hippocampus. Brain Behav. Immun. 1–15. http://dx.doi.org/10.1016/j.bbi.2016.06.006.

Derveaux, S., Vandesompele, J., Hellemans, J., 2010. How to do successful gene expression analysis using real-time PCR. Methods 50, 227–230. http://dx.doi.org/10.1016/j.ymeth.2009.11.001.

Diz-Chaves, Y., Astiz, M., Bellini, M.J., Garcia-Segura, L.M., 2013. Prenatal stress increases the expression of proinflammatory cytokines and exacerbates the inflammatory response to LPS in the hippocampal formation of adult male mice. Brain Behav. Immun. 28, 196–206. http://dx.doi.org/10.1016/j.bbi.2012.11.013.

Diz-Chaves, Y., Pernía, O., Carrero, P., Garcia-Segura, L.M., 2012. Prenatal stress causes alterations in the morphology of microglia and the inflammatory response of the hippocampus of adult female mice. J. Neuroinflammation 9, 71. http://dx.doi.org/10.1186/1742-2094-9-71.

do Prado, C.H., Narahari, T., Holland, F.H., Lee, H.-N., Murthy, S.K., Brenhouse, H.C., 2015. Effects of early adolescent environmental enrichment on cognitive dysfunction, prefrontal cortex development, and inflammatory cytokines after early life stress. Dev. Psychobiol. 58, 482–491. http://dx.doi.org/10.1002/dev.21390.

Dong, H., Yuede, C.M., Yoo, H.S., Martin, M.V., Deal, C., Mace, A.G., Csernansky, J.G., 2008. Corticosterone and related receptor expression are associated with increased beta-amyloid plaques in isolated Tg2576 mice. Neuroscience 155, 154–163. http://dx.doi.org/10.1016/j.neuroscience.2008.05.017.

Felderhoff-Mueser, U., Sifringer, M., Polley, O., Dzietko, M., Leineweber, B., Mahler, L., Baier, M., Bittigau, P., Obladen, M., Ikonomidou, C., Bührer, C., 2005. Caspase-1-processed interleukins in hyperoxia-induced cell death in the developing brain. Ann. Neurol. 57, 50–59. http://dx.doi.org/10.1002/ana.20322.

Ferretti, M.T., Bruno, M.A., Ducatenzeiler, A., Klein, W.L., Cuello, A.C., 2012. Intracellular Aβ-oligomers and early inflammation in a model of Alzheimer's disease. Neurobiol. Aging 33, 1329–1342. http://dx.doi.org/10.1016/j.neurobiolaging.2011.01.007.

Fu, H., Liu, B., Frost, J.L., Hong, S., Jin, M., Ostaszewski, B., Shankar, G.M., Costantino, I. M., Carroll, M.C., Mayadas, T.N., Lemere, C.A., 2012. Complement component C3 and complement receptor type 3 contribute to the phagocytosis and clearance of fibrillar Aβ by microglia. Glia 60, 993–1003. http://dx.doi.org/10.1002/glia.22331.

Garcia-Alloza, M., Robbins, E.M., Zhang-Nunes, S.X., Purcell, S.M., Betensky, R.A., Raju, S., Prada, C., Greenberg, S.M., Bacskai, B.J., Frosch, M.P., 2006. Characterization of amyloid deposition in the APPswe/PS1dE9 mouse model of Alzheimer disease. Neurobiol. Dis. 24, 516–524. http://dx.doi.org/10.1016/j.nbd.2006.08.017.

Gómez-González, B., Escobar, A., 2009. Prenatal stress alters microglial development and distribution in postnatal rat brain. Acta Neuropathol. 119, 303–315. http://dx.doi.org/10.1007/s00401-009-0590-4.

Green, K.N., Billings, L.M., Roozendaal, B., McGaugh, J.L., LaFerla, F.M., 2006. Glucocorticoids increase amyloid-beta and tau pathology in a mouse model of Alzheimer's disease. J. Neurosci. 26, 9047–9056. http://dx.doi.org/10.1523/JNEUROSCI.2797-06.2006.

Greter, M., Lelios, I., Croxford, A.L., 2015. Microglia versus myeloid cell nomenclature during brain inflammation. Front. Immunol. 6, 249. http://dx.doi.org/10.3389/fimmu.2015.00249.

Grigoryan, G., Biella, G., Albani, D., Forloni, G., Segal, M., 2014. Stress impairs synaptic plasticity in triple-transgenic Alzheimer's disease mice: rescue by ryanodine. Neurodegener. Dis. 13, 135–138. http://dx.doi.org/10.1159/000354231.

Giménez-Llort, L. et al., 2007. Modeling behavioral and neuronal symptoms of Alzheimer's disease in mice: a role for intraneuronal amyloid. Neurosci. Biobehav. Rev. 31, 125–147. http://dx.doi.org/10.1016/j.neubiorev.2006.07.007.

Guillot-Sestier, M.-V., Doty, K.R., Town, T., 2015. Innate immunity fights Alzheimer's disease. Trends Neurosci. 38, 674–681. http://dx.doi.org/10.1016/j.tins.2015.08.008.

Guo, H.B., Cheng, Y.F., Wu, J.G., Wang, C.M., Wang, H.T., Zhang, C., Qiu, Z.K., Xu, J.P., 2015. Donepezil improves learning and memory deficits in APP/PS1 mice by inhibition of microglial activation. Neuroscience 290, 530–542. http://dx.doi.org/10.1016/j.neuroscience.2015.01.058.

Han, B., Yu, L., Geng, Y., Shen, L., Wang, H., Wang, Y., Wang, J., Wang, M., 2016. Chronic stress aggravates cognitive impairment and suppresses insulin associated signaling pathway in APP/PS1 mice. J. Alzheimers Dis. 53, 1539–1552. http://dx.doi.org/10.3233/JAD-160189.

Harry, G.J., 2013. Microglia during development and aging. Pharmacol. Ther. 139, 313–326. http://dx.doi.org/10.1016/j.pharmthera.2013.04.013.

Hellemans, J., Mortier, G., De Paepe, A., Speleman, F., Vandesompele, J., 2007. QBase relative quantification framework and software for management and automated analysis of real-time quantitative PCR data. Genome Biol. 8, R19. http://dx.doi.org/10.1186/gb-2007-8-2-r19.

Heneka, M.T., Carson, M.J., Khoury, J.E., Landreth, G.E., Brosseron, F., Feinstein, D.L., Jacobs, A.H., Wyss-Coray, T., Vitorica, J., Ransohoff, R.M., Herrup, K., Frautschy, S. A., Finsen, B., Brown, G.C., Verkhratsky, A., Yamanaka, K., Koistinaho, J., Latz, E., Halle, A., Petzold, G.C., Town, T., Morgan, D., Shinohara, M.L., Perry, V.H., Holmes, C., Bazan, N.G., Brooks, D.J., Hunot, S., Joseph, B., Deigendesch, N.,

Garaschuk, O., Boddeke, E., Dinarello, C.A., Breitner, J.C., Cole, G.M., Golenbock, D.T., Kummer, M.P., 2015. Neuroinflammation in Alzheimer's disease. Lancet Neurol. 14, 388–405. http://dx.doi.org/10.1016/S1474-4422(15)70016-5.

Heppner, F.L., Ransohoff, R.M., Becher, B., 2015. Immune attack: the role of inflammation in Alzheimer disease. Nat. Neurosci. 16, 358–372. http://dx.doi.org/10.1038/nrn3880.

Hoeijmakers, L., Heinen, Y., Van Dam, A.M., Lucassen, P.J., Korosi, A., 2016. Microglial priming and Alzheimer's disease: a possible role for (early) immune challenges and epigenetics? Front. Hum. Neurosci. 10. http://dx.doi.org/10.3389/fnhum.2016.00398. 290–15.

Hoeijmakers, L., Korosi, A., Lucassen, P.J., 2015. The interplay of early-life stress, nutrition, and immune activation programs adult hippocampal structure and function. Front. Mol. Neurosci. 7, 1–16. http://dx.doi.org/10.3389/fnmol.2014.00103/abstract.

Hsiao, K.K., Borchelt, D.R., Olson, K., Johannsdottir, R., Kitt, C., Yunis, W., Xu, S., Eckman, C., Younkin, S., Price, D., 1995. Age-related CNS disorder and early death in transgenic FVB/N mice overexpressing Alzheimer amyloid precursor proteins. Neuron 15, 1203–1218. http://dx.doi.org/10.1016/0896-6273(95)90107-8.

Huang, H., Wang, L., Cao, M., Marshall, C., Gao, J., Xiao, N., Hu, G., Xiao, M., 2015. Isolation housing exacerbates Alzheimer's disease-like pathophysiology in aged APP/PS1 mice. Int. J. Neuropsychopharm. 18, 1–10. http://dx.doi.org/10.1093/ijnp/pyu116.

Jankowsky, J.L., Fadale, D.J., Anderson, J., Xu, G.M., Gonzales, V., Jenkins, N.A., Copeland, N.G., Lee, M.K., Younkin, L.H., Wagner, S.L., Younkin, S.G., Borchelt, D. R., 2004. Mutant presenilins specifically elevate the levels of the 42 residue beta-amyloid peptide in vivo: evidence for augmentation of a 42-specific gamma secretase. Hum. Mol. Genet. 13, 159–170. http://dx.doi.org/10.1093/hmg/ddh019.

Jaworski, T., Dewachter, I., Seymour, C.M., Borgraef, P., Devijver, H., Kügler, S., Van Leuven, F., 2010. Alzheimer's disease: Old problem, new views from transgenic and viral models. BBA-Mol. Basis Dis. 1802, 808–818. http://dx.doi.org/10.1016/j.bbadis.2010.03.005.

Jeong, Y.H., 2006. Chronic stress accelerates learning and memory impairments and increases amyloid deposition in APPV717I-CT100 transgenic mice, an Alzheimer's disease model. FASEB J. http://dx.doi.org/10.1096/fj.05-4265fje.

Johansson, L., Guo, X., Hällström, T., Norton, M.C., Waern, M., Östling, S., Bengtsson, C., Skoog, I., 2013. Common psychosocial stressors in middle-aged women related to longstanding distress and increased risk of Alzheimer's disease: a 38-year longitudinal population study. BMJ Open 3, e003142. http://dx.doi.org/10.1136/bmjopen-2013-003142.

Kaplan, G.A., Turrell, G., Lynch, J.W., Everson, S.A., Helkala, E.L., Salonen, J.T., 2001. Childhood socioeconomic position and cognitive function in adulthood. Int. J. Epidemiol. 30, 256–263. http://dx.doi.org/10.1093/ije/30.2.256.

Katz, M.J., Derby, C.A., Wang, C., Sliwinski, M.J., Ezzati, A., Zimmerman, M.E., Zwerling, J.L., Lipton, R.B., 2016. Influence of perceived stress on incident amnestic mild cognitive impairment: results from the einstein aging study. Alzheimer Dis. Assoc. Disord. 30, 93–98. http://dx.doi.org/10.1097/WAD.0000000000000125.

LaFerla, F.M., Green, K.N., Oddo, S., 2007. Intracellular amyloid-β in Alzheimer's disease. Nat. Rev. Neurosci. 8, 499–509. http://dx.doi.org/10.1038/nrn2168.

Lahiri, D.K., Maloney, B., 2012. The "LEARn" (latent early-life associated regulation) model: an epigenetic pathway linking metabolic and cognitive disorders. J. Alzheimers Dis. 30 (Suppl. 2), S15–S30. http://dx.doi.org/10.3233/JAD-2012-120373.

Lahiri, D.K., Maloney, B., 2010. The "LEARn" (Latent Early-life Associated Regulation) model integrates environmental risk factors and the developmental basis of Alzheimer's disease, and proposes remedial steps. Exp. Gerontol. 45, 291–296. http://dx.doi.org/10.1016/j.exger.2010.01.001.

Lee, S., Varvel, N.H., Konerth, M.E., Xu, G., Cardona, A.E., Ransohoff, R.M., Lamb, B.T., 2010. CX3CR1 deficiency alters microglial activation and reduces beta-amyloid deposition in two Alzheimer's disease mouse models. Am. J. Pathol. 177, 2549–2562. http://dx.doi.org/10.2353/ajpath.2010.100265.

Lesuis, S.L., Maurin, H., Borghgraef, P., Lucassen, P.J., Van Leuven, F., Krugers, H.J., 2016. Positive and negative early life experiences differentially modulate long term survival and amyloid protein levels in a mouse model of Alzheimer's disease. Oncotarget 7, 39118–39135. http://dx.doi.org/10.18632/oncotarget.9776.

Li, N., Wang, Y., Zhao, X., Gao, Y., Song, M., Yu, L., Wang, L., Li, N., Chen, Q., Li, Y., Cai, J., Wang, X., 2015. Long-term effect of early-life stress from earthquake exposure on working memory in adulthood. Neuropsychiatr. Dis. Treat. 11, 2959–2965. http://dx.doi.org/10.2147/NDT.S88770.

Liu, R., Yang, X.-D., Liao, X.-M., Xie, X.-M., Su, Y.-A., Li, J.-T., Wang, X.-D., Si, T.-M., 2016. Early postnatal stress suppresses the developmental trajectory of hippocampal pyramidal neurons: the role of CRHR1. Brain Struct. Funct. 1–12. http://dx.doi.org/10.1007/s00429-016-1182-4.

Liu, Z., Condello, C., Schain, A., Harb, R., Grutzendler, J., 2010. CX3CR1 in microglia regulates brain amyloid deposition through selective protofibrillar amyloid-β phagocytosis. J. Neurosci. 30, 17091–17101. http://dx.doi.org/10.1523/JNEUROSCI.4403-10.2010.

Lucassen, P.J., Naninck, E.F.G., Van Goudoever, J.B., Fitzsimons, C., Korosi, A., 2013. Perinatal programming of adult hippocampal structure and function; emerging roles of stress, nutrition and epigenetics. Trends Neurosci. 36, 621–631. http://dx.doi.org/10.1016/j.tins.2013.08.002.

Lupien, S.J., Nair, N., Briere, S., Maheu, F., Tu, M.T., Lemay, M., McEwen, B.S., Meaney, M.J., 1999. Increased cortisol levels and impaired cognition in human aging: implication for depression and dementia in later life. Rev. Neurosci. 10, 117–139. http://dx.doi.org/10.1515/REVNEURO.1999.10.2.117.

Machado, T.D., Salum, G.A., Bosa, V.L., Goldani, M.Z., Meaney, M.J., Agranonik, M., Manfro, G.G., Silveira, P.P., 2015. Early life trauma is associated with decreased peripheral levels of thyroid-hormone T3 in adolescents. Int. J. Dev. Neurosci. 47, 304–308. http://dx.doi.org/10.1016/j.ijdevneu.2015.10.005.

Majumdar, A., Cruz, D., Asamoah, N., Buxbaum, A., Sohar, I., Lobel, P., Maxfield, F.R., 2007. Activation of microglia acidifies lysosomes and leads to degradation of Alzheimer amyloid fibrils. Mol. Biol. Cell 18, 1490–1496. http://dx.doi.org/10.1091/mbc.E06-10-0975.

Malik, M., Parikh, I., Vasquez, J.B., Smith, C., Tai, L., Bu, G., LaDu, M.J., Fardo, D.W., Rebeck, G.W., Estus, S., 2015. Genetics ignite focus on microglial inflammation in Alzheimer's disease. Mol. Neurodegeneration 10, 1. http://dx.doi.org/10.1186/s13024-015-0048-1.

Marlatt, M.W., Potter, M.C., Bayer, T.A., van Praag, H., Lucassen, P.J., 2013. Prolonged running, not fluoxetine treatment, increases neurogenesis, but does not alter neuropathology, in the 3xTg mouse model of Alzheimer's disease. Curr. Top. Behav. Neurosci. 15, 313–340. http://dx.doi.org/10.1007/7854_2012_237.

Matcovitch-Natan, O., Winter, D.R., Giladi, A., Vargas Aguilar, S., Spinrad, A., Sarrazin, S., Ben-Yehuda, H., David, E., Zelada González, F., Perrin, P., Keren-Shaul, H., Gury, M., Lara-Astaiso, D., Thaiss, C.A., Cohen, M., Bahar Halpern, K., Baruch, K., Deczkowska, A., Lorenzo-Vivas, E., Itzkovitz, S., Elinav, E., Sieweke, M. H., Schwartz, M., Amit, I., 2016. Microglia development follows a stepwise program to regulate brain homeostasis. Science 353. http://dx.doi.org/10.1126/science.aad8670. aad8670–aad8670.

Mayeux, R., Stern, Y., 2012. Epidemiology of Alzheimer disease. Cold Spring Harb. Perspect. Med. 2, a006239. http://dx.doi.org/10.1101/cshperspect.a006239.

Meyer-Luehmann, M., Prinz, M., 2015. Myeloid cells in Alzheimer's disease: culprits, victims or innocent bystanders? Trends Neurosci. 38, 659–668. http://dx.doi.org/10.1016/j.tins.2015.08.011.

Mhatre, S.D., Tsai, C.A., Rubin, A.J., James, M.L., Andreasson, K.I., 2015. Microglial malfunction: the third rail in the development of Alzheimer's disease. Trends Neurosci. 38, 621–636. http://dx.doi.org/10.1016/j.tins.2015.08.006.

Mildner, A., Schlevogt, B., Kierdorf, K., Bottcher, C., Erny, D., Kummer, M.P., Quinn, M., Bruck, W., Bechmann, I., Heneka, M.T., Priller, J., Prinz, M., 2011. Distinct and non-redundant roles of microglia and myeloid subsets in mouse models of Alzheimer's disease. J. Neurosci. 31, 11159–11171. http://dx.doi.org/10.1523/JNEUROSCI.6209-10.2011.

Mishra, J., Gazzaley, A., 2014. Closed-loop rehabilitation of age-related cognitive disorders. Semin. Neurol. 34, 584–590. http://dx.doi.org/10.1055/s-0034-1396011.

Moechars, D., Lorent, K., Van Leuven, F., 1999. Premature death in transgenic mice that overexpress a mutant amyloid precursor protein is preceded by severe neurodegeneration and apoptosis. *Neuroscience* 91, 819–830. http://dx.doi.org/10.1016/S0306-4522(98)00599-5.

Mueller, S.C., Maheu, F.S., Dozier, M., Peloso, E., Mandell, D., Leibenluft, E., Pine, D.S., Ernst, M., 2010. Early-life stress is associated with impairment in cognitive control in adolescence: an fMRI study. Neuropsychologia 48, 3037–3044. http://dx.doi.org/10.1016/j.neuropsychologia.2010.06.013.

Naninck, E.F.G., Hoeijmakers, L., Kakava-Georgiadou, N., Meesters, A., Lazic, S.E., Lucassen, P.J., Korosi, A., 2015. Chronic early life stress alters developmental and adult neurogenesis and impairs cognitive function in mice. Hippocampus 25, 309–328. http://dx.doi.org/10.1002/hipo.22374.

Papageorgiou, I.E., Lewen, A., Galow, L.V., Cesetti, T., Scheffel, J., Regen, T., Hanisch, U.-K., Kann, O., 2016. TLR4-activated microglia require IFN-γ to induce severe neuronal dysfunction and death in situ. PNAS 113, 212–217. http://dx.doi.org/10.1073/pnas.1513853113.

Philip, N.S., Sweet, L.H., Tyrka, A.R., Carpenter, S.L., Albright, S.E., Price, L.H., Carpenter, L.L., 2015. Exposure to childhood trauma is associated with altered n-back activation and performance in healthy adults: implications for a commonly used working memory task. Brain Imaging Behav. 1–12. http://dx.doi.org/10.1007/s11682-015-9373-9.

Price, L.H., Kao, H.T., Burgers, D.E., Carpenter, L.L., Tyrka, A.R., 2013. Telomeres and early-life stress: an overview. Biol. Psychiat. 73, 15–23. http://dx.doi.org/10.1016/j.biopsych.2012.06.025.

Prinz, M., Priller, J., 2014. Microglia and brain macrophages in the molecular age: from origin to neuropsychiatric disease. Nat. Rev. Neurosci. 15, 300–312. http://dx.doi.org/10.1038/nrn3722.

Prinz, M., Priller, J., Sisodia, S.S., Ransohoff, R.M., 2011. Heterogeneity of CNS myeloid cells and their roles in neurodegeneration. Nat. Neurosci. 14, 1227–1235. http://dx.doi.org/10.1038/nn.2923.

Puoliväli, J., Wang, J., Heikkinen, T., Heikkilä, M., Tapiola, T., van Groen, T., Tanila, H., 2002. Hippocampal Aβ42 levels correlate with spatial memory deficit in APP and PS1 double transgenic mice. Neurobiol. Dis. 9, 339–347. http://dx.doi.org/10.1006/nbdi.2002.0481.

Querfurth, H.W., LaFerla, F.M., 2010. Alzheimer's disease. N. Engl. J. Med. 362, 329–344. http://dx.doi.org/10.1056/NEJMra0909142.

Ravona-Springer, R., Beeri, M.S., Goldbourt, U., 2012. Younger age at crisis following parental death in male children and adolescents is associated with higher risk for dementia at old age. Alzheimer Dis. Assoc. Disord. 26, 68–73. http://dx.doi.org/10.1097/WAD.0b013e3182191f86.

Redlich, R., Stacey, D., Opel, N., Grotegerd, D., Dohm, K., Kugel, H., Heindel, W., Arolt, V., Baune, B.T., Dannlowski, U., 2015. Evidence of an IFN-γ by early life stress interaction in the regulation of amygdala reactivity to emotional stimuli. Psychoneuroendocrino. 62, 166–173. http://dx.doi.org/10.1016/j.psyneuen.2015.08.008.

Reemst, K., Noctor, S.C., Lucassen, P.J., Hol, E., 2016. The indispensable roles of microglia and astrocytes during brain development. Front. Hum. Neurosci. 10, 566. http://dx.doi.org/10.3389/fnhum.2016.00566.

Reitz, C., Mayeux, R., 2014. Alzheimer disease: epidemiology, diagnostic criteria, risk factors and biomarkers. Biochem. Pharmacol. 88, 640–651. http://dx.doi.org/10.1016/j.bcp.2013.12.024.

Rice, C.J., Sandman, C.A., Lenjavi, M.R., Baram, T.Z., 2008. A novel mouse model for acute and long-lasting consequences of early life stress. Endocrinology 149, 4892–4900. http://dx.doi.org/10.1210/en.2008-0633.

Roque, A., Ochoa-Zarzosa, A., Torner, L., 2016. Maternal separation activates microglial cells and induces an inflammatory response in the hippocampus of male rat pups, independently of hypothalamic and peripheral cytokine levels. Brain Behav. Immun. 55, 39–48. http://dx.doi.org/10.1016/j.bbi.2015.09.017.

Roque, S., Mesquita, A.R., Palha, J.A., Sousa, N., Correia-Neves, M., 2014. The behavioral and immunological impact of maternal separation: a matter of timing. Front. Behav. Neurosci. 8, 192. http://dx.doi.org/10.3389/fnbeh.2014.00192.

Rothman, S.M., Herdener, N., Camandola, S., Texel, S.J., Mughal, M.R., Cong, W.-N., Martin, B., Mattson, M.P., 2012. 3xTgAD mice exhibit altered behavior and elevated Aβ after chronic mild social stress. Neurobiol. Aging 33 (830), e1–e12. http://dx.doi.org/10.1016/j.neurobiolaging.2011.07.005.

Schury, K., Kolassa, I.-T., 2012. Biological memory of childhood maltreatment: current knowledge and recommendations for future research. Ann. N. Y. Acad. Sci. 1262, 93–100. http://dx.doi.org/10.1111/j.1749-6632.2012.06617.x.

Schwarz, J.M., Bilbo, S.D., 2012. Sex, glia, and development: interactions in health and disease. Horm. Behav. 62, 243–253. http://dx.doi.org/10.1016/j.yhbeh.2012.02.018.

Schwarz, J.M., Sholar, P.W., Bilbo, S.D., 2012. Sex differences in microglial colonization of the developing rat brain. J. Neurochem. 120, 948–963. http://dx.doi.org/10.1111/j.1471-4159.2011.07630.x.

Sierksma, A.S.R., Prickaerts, J., Chouliaras, L., Rostamian, S., Delbroek, L., Rutten, B.P.F., Steinbusch, H.W.M., van den Hove, D.L.A., 2013. Behavioral and neurobiological effects of prenatal stress exposure in male and female APPswe/PS1dE9 mice. Neurobiol. Aging 34, 319–337. http://dx.doi.org/10.1016/j.neurobiolaging.2012.05.012.

Sierksma, A.S.R., Vanmierlo, T., De Vry, J., Raijmakers, M.E.A., Steinbusch, H.W.M., van den Hove, D.L.A., Prickaerts, J., 2012. Effects of prenatal stress exposure on soluble Aβ and brain-derived neurotrophic factor signaling in male and female APPswe/PS1dE9 mice. Neurochem. Int. 61, 697–701. http://dx.doi.org/10.1016/j.neuint.2012.06.022.

Simard, A.R., Soulet, D., Gowing, G., Julien, J.-P., Rivest, S., 2006. bone marrow-derived microglia play a critical role in restricting senile plaque formation in Alzheimer's disease. Neuron 49, 489–502. http://dx.doi.org/10.1016/j.neuron.2006.01.022.

Ślusarczyk, J., Trojan, E., Głombik, K., Budziszewska, B., Kubera, M., Lasoń, W., Popiołek-Barczyk, K., Mika, J., Wędzony, K., Basta-Kaim, A., 2015. Prenatal stress is a vulnerability factor for altered morphology and biological activity of microglia cells. Front. Cell. Neurosci. 9, 1–14. http://dx.doi.org/10.3389/fncel.2015.00082.

Spangenberg, E.E., Green, K.N., 2017. Inflammation in Alzheimer's disease: lessons learned from microglia-depletion models. Brain Behav. Immun. 61, 1–11.

Szczesny, E., Basta-Kaim, A., Ślusarczyk, J., Trojan, E., Glombik, K., Regulska, M., Leśkiewicz, M., Budziszewska, B., Kubera, M., Lason, W., 2014. The impact of prenatal stress on insulin-like growth factor-1 and pro-inflammatory cytokine expression in the brains of adult male rats: the possible role of suppressors of cytokine signaling proteins. J. Neuroimmunol. 276, 37–46. http://dx.doi.org/10.1016/j.jneuroim.2014.08.001.

Trinchese, F., Liu, S., Battaglia, F., Walter, S., Mathews, P.M., Arancio, O., 2004. Progressive age-related development of Alzheimer-like pathology in APP/PS1 mice. Ann. Neurol. 55, 801–814. http://dx.doi.org/10.1002/ana.20101.

Tyrka, A.R., Parade, S.H., Valentine, T.R., Eslinger, N.M., Seifer, R., 2015. Adversity in preschool-aged children: effects on salivary interleukin-1β. Dev. Psychobiol. 27, 567–576. http://dx.doi.org/10.1017/S0954579415000164.

Tyrka, A.R., Price, L.H., Kao, H.-T., Porton, B., Marsella, S.A., Carpenter, L.L., 2010. Childhood maltreatment and telomere shortening: preliminary support for an effect of early stress on cellular aging. Biol. Psychiat. 67, 531–534. http://dx.doi.org/10.1016/j.biopsych.2009.08.014.

Vallee, M., Maccari, S., Dellu, F., Simon, H., Le Moal, M., Mayo, W., 1999. Long-term effects of prenatal stress and postnatal handling on age-related glucocorticoid secretion and cognitive performance: a longitudinal study in the rat. Eur. J. Neurosci. 11, 2906–2916. http://dx.doi.org/10.1046/j.1460-9568.1999.00705.x.

Vela, J., 2002. Interleukin-1 regulates proliferation and differentiation of oligodendrocyte progenitor cells. Mol. Cell. Neurosci. 20, 489–502. http://dx.doi.org/10.1006/mcne.2002.1127.

Wang, X.-D., Su, Y.-A., Wagner, K.V., Avrabos, C., Scharf, S.H., Hartmann, J., Wolf, M., Liebl, C., Kühne, C., Wurst, W., Holsboer, F., Eder, M., Deussing, J.M., Müller, M.B., Schmidt, M.V., 2013. Nectin-3 links CRHR1 signaling to stress-induced memory deficits and spine loss. Nat. Neurosci. 16, 706–713. http://dx.doi.org/10.1038/nn.3395.

Wang, Y., Cella, M., Mallinson, K., Ulrich, J.D., Young, K.L., Robinette, M.L., Gilfillan, S., Krishnan, G.M., Sudhakar, S., Zinselmeyer, B.H., Holtzman, D.M., Cirrito, J.R., Colonna, M., 2015. TREM2 lipid sensing sustains the microglial response in an Alzheimer's disease model. Cell 160, 1061–1071. http://dx.doi.org/10.1016/j.cell.2015.01.049.

Wang, Y., Ulland, T.K., Ulrich, J.D., Song, W., Tzaferis, J.A., Hole, J.T., Yuan, P., Mahan, T.E., Shi, Y., Gilfillan, S., Cella, M., Grutzendler, J., DeMattos, R.B., Cirrito, J.R., Holtzman, D.M., Colonna, M., 2016. TREM2-mediated early microglial response limits diffusion and toxicity of amyloid plaques. J. Exp. Med. 213, 667–675. http://dx.doi.org/10.1084/jem.20151948.

Wilson, R.S., Evans, D.A., Bienias, J.L., de Leon, C.F.M., Schneider, J.A., Bennett, D.A., 2003. Proneness to psychological distress is associated with risk of Alzheimer's disease. Neurology 61, 1479–1485. http://dx.doi.org/10.1212/01.WNL.0000096167.56734.59.

Wolkowitz, O.M., Epel, E.S., Reus, V.I., Mellon, S.H., 2010. Depression gets old fast: do stress and depression accelerate cell aging? Depress Anxiety 27, 327–338. http://dx.doi.org/10.1002/da.20686.

Yu, Y., He, J., Zhang, Y., Luo, H., Zhu, S., Yang, Y., Zhao, T., Wu, J., Huang, Y., Kong, J., Tan, Q., Li, X.-M., 2009. Increased hippocampal neurogenesis in the progressive stage of Alzheimer's disease phenotype in an APP/PS1 double transgenic mouse model. Hippocampus 19, 1247–1253. http://dx.doi.org/10.1002/hipo.20587.

Zhang, W., Hao, J., Liu, R., Zhang, Z., Lei, G., Su, C., Miao, J., Li, Z., 2011. Soluble Aβ levels correlate with cognitive deficits in the 12-month-old APPswe/PS1dE9 mouse model of Alzheimer's disease. Behav. Brain Res. 222, 342–350. http://dx.doi.org/10.1016/j.bbr.2011.03.072.

Zhang, W., Bai, M., Xi, Y., Hao, J., Zhang, Z., Su, C., Lei, G., Miao, J., Li, Z., 2012. Multiple inflammatory pathways are involved in the development and progression of cognitive deficits in APPswe/PS1dE9 mice. Neurobiol. Aging 33, 2661–2677. http://dx.doi.org/10.1016/j.neurobiolaging.2011.12.023.

Ziko, I., De Luca, S., Dinan, T., Barwood, J.M., Sominsky, L., Cai, G., Kenny, R., Stokes, L., Jenkins, T.A., Spencer, S.J., 2014. Neonatal overfeeding alters hypothalamic microglial profiles and central responses to immune challenge long-term. Brain Behav. Immun. 41, 32–43. http://dx.doi.org/10.1016/j.bbi.2014.06.014.